A Systematic Study of Neutrino Mixing and CP Violation from Lepton Mass Matrices with Six Texture Zeros

Shun Zhou and **Zhi-zhong Xing**
CCAST (World Laboratory), P.O. Box 8730, Beijing 100080, China
and Institute of High Energy Physics, Chinese Academy of Sciences,
P.O. Box 918 (4), Beijing 100049, China
(Electronic address: xingzz@mail.ihep.ac.cn)

Abstract

We present a systematic study of 400 combinations of the charged lepton and neutrino mass matrices with six vanishing entries or texture zeros. Only 24 of them, which can be classified into a few distinct categories, are found to be compatible with current neutrino oscillation data at the 3σ level. A peculiar feature of the lepton mass matrices in each category is that they have the same phenomenological consequences. Taking account of a simple seesaw scenario for six parallel patterns of the charged lepton and Dirac neutrino mass matrices with six zeros, we show that it is possible to fit the experimental data at or below the 2σ level. In particular, the maximal atmospheric neutrino mixing can be reconciled with a strong neutrino mass hierarchy in the seesaw case. Numerical predictions are also obtained for the neutrino mass spectrum, flavor mixing angles, CP-violating phases and effective masses of the tritium beta decay and the neutrinoless double beta decay.

PACS number(s): 12.15.Ff, 12.10.Kt

I. INTRODUCTION

Recent solar [1], atmospheric [2], reactor (KamLAND [3] and CHOOZ [4]) and accelerator (K2K [5]) neutrino oscillation experiments have provided us with very convincing evidence that neutrinos are massive and lepton flavors are mixed. In the framework of three lepton families, a full description of the lepton mass spectra and flavor mixing at low energies needs twelve physical parameters:

- three charged lepton masses m_e, m_μ and m_τ, which have precisely been measured [6];
- three neutrino masses m_1, m_2 and m_3, whose relative sizes (i.e., two independent mass-squared differences $\Delta m^2_{21} \equiv m^2_2 - m^2_1$ and $\Delta m^2_{31} \equiv m^2_3 - m^2_1$) have roughly been known from solar ($\Delta m^2_{21} \sim 10^{-5}$ eV^2) and atmospheric ($|\Delta m^2_{31}| \sim 10^{-3}$ eV^2) neutrino oscillations;
- three flavor mixing angles θ_{12}, θ_{23} and θ_{13}, whose values have been determined or constrained to an acceptable degree of accuracy from solar ($\theta_{12} \sim 33^\circ$), atmospheric ($\theta_{23} \sim 45^\circ$) and reactor ($\theta_{13} < 13^\circ$) neutrino oscillations;
- three CP-violating phases δ, ρ and σ, which are completely unrestricted by current neutrino data.

The future neutrino oscillation experiments are expected to fix the sign of Δm^2_{31}, to pin down the magnitude of θ_{13} and to probe the "Dirac-type" CP-violating phase δ. The proposed precision experiments for the tritium beta decay and the neutrinoless double beta decay will help determine or constrain the absolute scale of three neutrino masses. Some information about the "Majorana-type" CP-violating phases ρ and σ may also be achieved from a delicate measurement of the neutrinoless double beta decay. However, it seems hopeless to separately determine ρ and σ from any conceivable sets of feasible neutrino experiments in the foreseeable future.

The phenomenology of lepton masses and flavor mixing at low energies can be formulated in terms of the charged lepton mass matrix M_l and the (effective) neutrino mass matrix M_ν. While the former is in general arbitrary, the latter must be a symmetric matrix required by the Majorana nature of three neutrino fields. Hence we diagonalize M_l by using two unitary matrices and M_ν by means of a single unitary matrix:

$$\begin{aligned} U^\dagger_l M_l \hat{U}_l &= \begin{pmatrix} m_e & 0 & 0 \\ 0 & m_\mu & 0 \\ 0 & 0 & m_\tau \end{pmatrix} , \\ U^\dagger_\nu M_\nu U^*_\nu &= \begin{pmatrix} m_1 & 0 & 0 \\ 0 & m_2 & 0 \\ 0 & 0 & m_3 \end{pmatrix} . \end{aligned} \tag{1}$$

The lepton flavor mixing matrix V is defined as $V \equiv U^\dagger_l U_\nu$, which describes the mismatch between the diagonalizations of M_l and M_ν. In the flavor basis where M_l is diagonal and positive, V directly links the neutrino mass eigenstates (ν_1, ν_2, ν_3) to the neutrino flavor eigenstates $(\nu_e, \nu_\mu, \nu_\tau)$:

$$\begin{pmatrix} \nu_e \\ \nu_\mu \\ \nu_\tau \end{pmatrix} = \begin{pmatrix} V_{e1} & V_{e2} & V_{e3} \\ V_{\mu 1} & V_{\mu 2} & V_{\mu 3} \\ V_{\tau 1} & V_{\tau 2} & V_{\tau 3} \end{pmatrix} \begin{pmatrix} \nu_1 \\ \nu_2 \\ \nu_3 \end{pmatrix} \; . \tag{2}$$

A convenient parametrization of V is

$$V = \begin{pmatrix} c_{12}c_{13} & s_{12}c_{13} & s_{13} \\ -c_{12}s_{23}s_{13} - s_{12}c_{23}e^{-i\delta} & -s_{12}s_{23}s_{13} + c_{12}c_{23}e^{-i\delta} & s_{23}c_{13} \\ -c_{12}c_{23}s_{13} + s_{12}s_{23}e^{-i\delta} & -s_{12}c_{23}s_{13} - c_{12}s_{23}e^{-i\delta} & c_{23}c_{13} \end{pmatrix} \begin{pmatrix} e^{i\rho} & 0 & 0 \\ 0 & e^{i\sigma} & 0 \\ 0 & 0 & 1 \end{pmatrix} \; , \tag{3}$$

where $c_{ij} \equiv \cos\theta_{ij}$ and $s_{ij} \equiv \sin\theta_{ij}$ (for $ij = 12, 23, 13$). We have known that $\theta_{23} > \theta_{12} > \theta_{13}$ holds, but how small θ_{13} is remains an open question. A global analysis of current neutrino oscillation data shows that θ_{13} is most likely to lie in the range $4^\circ \leq \theta_{13} \leq 6^\circ$ [7]. In this case, we are left with a *bi-large* mixing pattern of V, which is quite different from the *tri-small* mixing pattern of the quark flavor mixing matrix.

To interpret the observed hierarchy of Δm^2_{21} and Δm^2_{31} as well as the bi-large lepton flavor mixing pattern, many phenomenological ansätze of lepton mass matrices have been proposed in the literature [8]. A very interesting category of the ansätze focus on the vanishing entries or *texture zeros* of M_l and M_ν in a specific flavor basis, from which some nontrivial and testable relations can be established between the flavor mixing parameters and the lepton mass ratios. We argue that texture zeros of lepton mass matrices might result from a kind of new (Abelian or non-Abelian) flavor symmetry beyond the standard electroweak model. Such zeros may dynamically mean that the corresponding matrix elements are sufficiently suppressed in comparison with their neighboring counterparts. From a phenomenological point of view, the study of possible texture zeros of M_l and M_ν at low energies *do* make sense, because it ought to help reveal the underlying structures of leptonic Yukawa couplings at a superhigh energy scale.

The main purpose of this article is to analyze the six-zero textures of M_l and M_ν in a systematic way. To be specific, we take M_l to be symmetric, just as M_ν is. This point is true in a number of SO(10) grand unification models, in which the group symmetry itself may dictate all fermion mass matrices to be symmetric [9]. Then a pair of off-diagonal texture zeros in M_l or M_ν can be counted as one zero. We further require that each mass matrix contain three texture zeros, such that the moduli of its three non-vanishing elements can fully be determined in terms of its three mass eigenvalues [1]. Because there exist 20 different

[1] One may certainly consider the possibility that one mass matrix contains two zeros and the other consists of four zeros. In this case, the former loses the calculability – namely, its four independent moduli cannot completely be calculated in terms of its three mass eigenvalues; and the latter causes the correlation between one of its three mass eigenvalues with the other two – this kind of mass correlation is in general incompatible with the relevant experimental data. One must reject the possibility that one mass matrix consists of one zero and the other contains five zeros, because the latter only has a single non-vanishing mass eigenvalue and is in strong conflict with our current knowledge about the charged lepton or neutrino masses. Therefore, we restrict ourselves to the most interesting and feasible case: six texture zeros are equally shared between M_l and M_ν.

patterns of M_l or M_ν with three texture zeros, we totally obtain $20 \times 20 = 400$ combinations of M_l and M_ν with six texture zeros. A careful analysis shows that only 24 of them, which can be classified into a few distinct categories, are consistent with current neutrino oscillation data at the 3σ level. We find that the lepton mass matrices in each category have a peculiar feature: they do not have the same structures, but their phenomenological consequences are exactly the same. This *isomeric* character makes the six-zero textures of lepton mass matrices especially interesting for model building. It is noticed that those 24 patterns of M_l and M_ν are difficult to agree with today's experimental data at the 2σ level, mainly due to a potential tension between the smallness of $\Delta m^2_{21}/|\Delta m^2_{31}|$ and the largeness of $\sin^2\theta_{23}$. Taking account of a very simple seesaw scenario for six parallel patterns of the charged lepton and Dirac neutrino mass matrices with six zeros, we demonstrate that it is possible to fit the present neutrino data at or below the 2σ level. In particular, the maximal atmospheric neutrino mixing (i.e., $\sin^2 2\theta_{23} \approx 1$) can be reconciled with a strong neutrino mass hierarchy in the seesaw case. Specific numerical predictions are also obtained for the neutrino mass spectrum, flavor mixing angles, CP-violating phases and effective masses of the tritium beta decay and the neutrinoless double beta decay.

The remaining part of this article is organized as follows. A classification of the six-zero textures of lepton mass matrices is presented in section II, where a few criteria to select the phenomenologically favorable patterns of M_l and M_ν are also outlined. Section III is devoted to the analytical and numerical calculations of 24 patterns of lepton mass matrices with or without the structural parallelism between M_l and M_ν. A simple application of the seesaw mechanism to the charged lepton and Dirac neutrino mass matrices with six texture zeros is illustrated in section IV. Finally, we summarize our main results in section V.

II. A CLASSIFICATION OF THE SIX-ZERO TEXTURES

A symmetric lepton mass matrix M (i.e., M_l or M_ν) has six independent entries. If three of them are taken to be vanishing, we totally arrive at

$$^6\mathbf{C}_3 = \frac{6!}{3!\,(6-3)!} = 20 \tag{4}$$

patterns, which are structurally different from one another. These twenty patterns of M can be classified into four categories:

1. Three diagonal matrix elements of M are all vanishing (type 0):

$$M_0 = \begin{pmatrix} \mathbf{0} & \times & \times \\ \times & \mathbf{0} & \times \\ \times & \times & \mathbf{0} \end{pmatrix} , \tag{5}$$

   where those non-vanishing entries are simply symbolized by $\times$'s.

2. Two diagonal matrix elements of M are vanishing (type I):

$$M_{\rm I_1} = \begin{pmatrix} {\bf 0} & \times & {\bf 0} \\ \times & {\bf 0} & \times \\ {\bf 0} & \times & \times \end{pmatrix} , \quad M_{\rm I_2} = \begin{pmatrix} {\bf 0} & {\bf 0} & \times \\ {\bf 0} & \times & \times \\ \times & \times & {\bf 0} \end{pmatrix} , \quad M_{\rm I_3} = \begin{pmatrix} {\bf 0} & \times & \times \\ \times & {\bf 0} & {\bf 0} \\ \times & {\bf 0} & \times \end{pmatrix} ,$$
$$M_{\rm I_4} = \begin{pmatrix} {\bf 0} & \times & \times \\ \times & \times & {\bf 0} \\ \times & {\bf 0} & {\bf 0} \end{pmatrix} , \quad M_{\rm I_5} = \begin{pmatrix} \times & {\bf 0} & \times \\ {\bf 0} & {\bf 0} & \times \\ \times & \times & {\bf 0} \end{pmatrix} , \quad M_{\rm I_6} = \begin{pmatrix} \times & \times & {\bf 0} \\ \times & {\bf 0} & \times \\ {\bf 0} & \times & {\bf 0} \end{pmatrix} , \tag{6}$$

which are of rank three; and

$$M_{\rm I_7} = \begin{pmatrix} {\bf 0} & {\bf 0} & \times \\ {\bf 0} & {\bf 0} & \times \\ \times & \times & \times \end{pmatrix} , \quad M_{\rm I_8} = \begin{pmatrix} {\bf 0} & \times & {\bf 0} \\ \times & \times & \times \\ {\bf 0} & \times & {\bf 0} \end{pmatrix} , \quad M_{\rm I_9} = \begin{pmatrix} \times & \times & \times \\ \times & {\bf 0} & {\bf 0} \\ \times & {\bf 0} & {\bf 0} \end{pmatrix} , \tag{7}$$

which are of rank two.

3. One diagonal matrix element of M is vanishing (type II):

$$M_{\rm II_1} = \begin{pmatrix} \times & \times & {\bf 0} \\ \times & {\bf 0} & {\bf 0} \\ {\bf 0} & {\bf 0} & \times \end{pmatrix} , \quad M_{\rm II_2} = \begin{pmatrix} \times & {\bf 0} & \times \\ {\bf 0} & \times & {\bf 0} \\ \times & {\bf 0} & {\bf 0} \end{pmatrix} , \quad M_{\rm II_3} = \begin{pmatrix} {\bf 0} & \times & {\bf 0} \\ \times & \times & {\bf 0} \\ {\bf 0} & {\bf 0} & \times \end{pmatrix} ,$$
$$M_{\rm II_4} = \begin{pmatrix} {\bf 0} & {\bf 0} & \times \\ {\bf 0} & \times & {\bf 0} \\ \times & {\bf 0} & \times \end{pmatrix} , \quad M_{\rm II_5} = \begin{pmatrix} \times & {\bf 0} & {\bf 0} \\ {\bf 0} & \times & \times \\ {\bf 0} & \times & {\bf 0} \end{pmatrix} , \quad M_{\rm II_6} = \begin{pmatrix} \times & {\bf 0} & {\bf 0} \\ {\bf 0} & {\bf 0} & \times \\ {\bf 0} & \times & \times \end{pmatrix} , \tag{8}$$

which are of rank three; and

$$M_{\rm II_7} = \begin{pmatrix} \times & \times & {\bf 0} \\ \times & \times & {\bf 0} \\ {\bf 0} & {\bf 0} & {\bf 0} \end{pmatrix} , \quad M_{\rm II_8} = \begin{pmatrix} \times & {\bf 0} & \times \\ {\bf 0} & {\bf 0} & {\bf 0} \\ \times & {\bf 0} & \times \end{pmatrix} , \quad M_{\rm II_9} = \begin{pmatrix} {\bf 0} & {\bf 0} & {\bf 0} \\ {\bf 0} & \times & \times \\ {\bf 0} & \times & \times \end{pmatrix} , \tag{9}$$

which are of rank two.

4. Three diagonal matrix elements of M are all non-vanishing (type III):

$$M_{\rm III} = \begin{pmatrix} \times & {\bf 0} & {\bf 0} \\ {\bf 0} & \times & {\bf 0} \\ {\bf 0} & {\bf 0} & \times \end{pmatrix} . \tag{10}$$

We see that M_0 and $M_{\rm I_1}$ are the well-known Zee [10] and Fritzsch [11] patterns of fermion mass matrices, respectively. Both of them are disfavored in the quark sector [12]. While the original Zee ansatz is also problematic in describing lepton masses and flavor mixing [13], the Fritzsch ansatz is found to be essentially compatible with current neutrino oscillation data [14].

Allowing the charged lepton or neutrino mass matrix to take one of the above three-zero textures, we totally have $20 \times 20 = 400$ combinations of M_l and M_ν. We find that 141 of them can easily be ruled out. First, the pattern in Eq. (5) is not suitable for M_l, because

three charged leptons have a strong mass hierarchy and the sum of their masses (i.e., the trace of M_ν) cannot be zero. Second, the rank-two patterns in Eqs. (7) and (9) are not suitable for M_l, because the former must have one vanishing mass eigenvalue. Third, M_l and M_ν cannot simultaneously take the pattern in Eq. (10), otherwise there would be no lepton flavor mixing. We are therefore left with $(20-7)\times 20-1=259$ combinations of M_l and M_ν.

To pick out the phenomenologically favorable six-zero patterns of lepton mass matrices from 259 combinations of M_l and M_ν, one has to confront their concrete predictions for the lepton mass spectra and flavor mixing angles with current neutrino oscillation data. The strategies to do so are outlined below:

1. For each combination of M_l and M_ν, we do the diagonalization like Eq. (1). Because M_l has been specified to be symmetric, $\hat{U}_l = U_l^*$ must hold. The matrix elements of U_l can be given in terms of two mass ratios ($x_l \equiv m_e/m_\mu \approx 0.00484$ and $y_l \equiv m_\mu/m_\tau \approx 0.0594$ [6]) and two irremovable phase parameters [2]. A similar treatment is applicable for the neutrino sector. The ratio of two independent neutrino mass-squared differences reads

$$R_\nu \equiv \left|\frac{\Delta m^2_{21}}{\Delta m^2_{31}}\right| = y_\nu^2 \, \frac{1-x_\nu^2}{|1-x_\nu^2 y_\nu^2|} \; , \tag{11}$$

   where $x_\nu \equiv m_1/m_2$ and $y_\nu \equiv m_2/m_3$. Note that $x_\nu < 1$ (i.e., $m_1 < m_2$) must hold, but it remains unclear whether $y_\nu < 1$ (normal mass hierarchy) or $y_\nu > 1$ (inverted mass hierarchy). The numerical results for Δm^2_{21} and $|\Delta m^2_{31}|$, which are obtained from a global analysis of current neutrino oscillation data [15], have been listed in Table I. We are therefore able to figure out the allowed range of R_ν.

2. The lepton flavor mixing matrix $V = U_l^\dagger U_\nu$ can then be obtained. Its nine elements depend on four mass ratios (x_l , y_l , x_ν and y_ν) and two irremovable phase combinations, which will subsequently be denoted as α and β. In the standard parametrization of V, as shown in Eq. (2), one has

$$\begin{aligned} \sin^2\theta_{12} &= \frac{|V_{e2}|^2}{1-|V_{e3}|^2} \; , \\ \sin^2\theta_{23} &= \frac{|V_{\mu 3}|^2}{1-|V_{e3}|^2} \; , \\ \sin^2\theta_{13} &= |V_{e3}|^2 \; . \end{aligned} \tag{12}$$

   The experimental results for $\sin^2\theta_{12}$, $\sin^2\theta_{23}$ and $\sin^2\theta_{13}$ are also listed in Table I.

---

[2] Without loss of generality, we can always arrange one of the three non-vanishing entries of M_l (or M_ν) to be positive. We are then left with two free phase parameters in M_l (or M_ν).

3. With the help of current experimental data, we make use of Eqs. (11) and (12) to look for the parameter space of each pattern of lepton mass matrices. The relevant free parameters include two neutrino mass ratios (x_ν and y_ν) and two CP-violating phases (α and β). The latter may in general vary between 0 and 2π. In our numerical analysis the points of x_ν, y_ν, α and β will be generated by scanning their possible ranges according to a flat random number distribution. Thus the density of output points in the (x_ν, y_ν) and (α, β) plots will be a clear reflection of strong constraints, imposed by the neutrino oscillation data and the model (or ansatz) itself, on these parameters. A combination of M_l and M_ν will be rejected, if its parameter space is found to be empty.

Of course, whether the parameter space of a specific pattern of lepton mass matrices is empty or not depends on the confidence levels of relevant experimental data. We shall focus on the 2σ and 3σ intervals of Δm^2_{21}, Δm^2_{31}, $\sin^2\theta_{12}$, $\sin^2\theta_{23}$ and $\sin^2\theta_{13}$ given in Ref. [15]. It is worth mentioning that a plain scan of the unknown parameters (x_ν, y_ν) and (α, β) is empirically simple and conservative, provided the reasonable ranges of Δm^2_{21} *etc* have been fixed. In this approximation the error bars of those observables need not be statistically treated.

Examining all 259 combinations of the charged lepton and neutrino mass matrices is a lengthy but straightforward work. We find that only 24 of them, whose M_l and M_ν both belong to type I given in Eqs. (6) and (7), are compatible with current neutrino oscillation data at the 3σ level. The detailed analytical and numerical calculations of those 24 patterns will be presented in sections III and IV.

Once the parameter space of a given pattern of lepton mass matrices is fixed, one may obtain some predictions for the neutrino mass spectrum and leptonic CP violation. For example, the absolute values of three neutrino masses can be determined as follows:

$$\begin{aligned} m_3 &= \frac{1}{\sqrt{|1-y_\nu^2|}} \sqrt{\Delta m^2_{\rm atm}} \; , \\ m_2 &= \frac{y_\nu}{\sqrt{|1-y_\nu^2|}} \sqrt{\Delta m^2_{\rm atm}} \; = \; \frac{1}{\sqrt{1-x_\nu^2}} \sqrt{\Delta m^2_{\rm sun}} \; , \\ m_1 &= \frac{x_\nu}{\sqrt{1-x_\nu^2}} \sqrt{\Delta m^2_{\rm sun}} \; . \end{aligned} \tag{13}$$

Three CP-violating phases in the standard parametrization of V are also calculable. As for CP violation in neutrino-neutrino or antineutrino-antineutrino oscillations, its strength is measured by the Jarlskog invariant $\mathcal{J}$ [16]. The definition of $\mathcal{J}$ reads

$$\mathrm{Im}\left(V_{ai} V_{bj} V^*_{aj} V^*_{bi}\right) \; = \; \mathcal{J} \sum_{c,k} \left(\epsilon_{abc} \epsilon_{ijk}\right) \; , \tag{14}$$

where the subscripts (a, b, c) and (i, j, k) run respectively over (e, μ, τ) and $(1, 2, 3)$. The magnitude of $\mathcal{J}$ depends on both (x_ν, y_ν) and (α, β). If $|\mathcal{J}| \sim 1\%$ is achievable, then leptonic CP- and T-violating effects could be measured in a variety of long-baseline neutrino oscillation experiments [17] in the future.

In addition, interesting predictions can be achieved for the effective mass of the tritium beta decay $\langle m \rangle_e$ and that of the neutrinoless double beta decay $\langle m \rangle_{ee}$:

$$\langle m \rangle_e^2 \equiv \sum_{i=1}^{3} \left(m_i^2 |V_{ei}|^2 \right) = m_3^2 \left(x_\nu^2 y_\nu^2 |V_{e1}|^2 + y_\nu^2 |V_{e2}|^2 + |V_{e3}|^2 \right) ,$$
$$\langle m \rangle_{ee} \equiv \left| \sum_{i=1}^{3} \left(m_i V_{ei}^2 \right) \right| = m_3 \left| x_\nu y_\nu V_{e1}^2 + y_\nu V_{e2}^2 + V_{e3}^2 \right| . \tag{15}$$

The present experimental upper bound on $\langle m \rangle_e$ is $\langle m \rangle_e < 2.2$ eV [6], while the sensitivity of the proposed KATRIN experiment is expected to reach $\langle m \rangle_e \sim 0.3$ eV [18]. In comparison, the upper limit $\langle m \rangle_{ee} < 0.35$ eV has been set by the Heidelberg-Moscow Collaboration [19] at the 90% confidence level [3]. The sensitivity of the next-generation experiments for the neutrinoless double beta decay is possible to reach $\langle m \rangle_{ee} \sim 10$ meV to 50 meV [21].

III. FAVORED PATTERNS OF LEPTON MASS MATRICES

The 24 patterns of lepton mass matrices, which are found to be compatible with current neutrino oscillation data at the 3σ level, all belong to the type-I textures listed in Eqs. (6) and (7). To make our subsequent discussions more convenient and concrete, we rewrite those type-I textures of M_l or M_ν and list them in Table II. Two comments are in order.

- Each type-I texture of M (i.e., M_l or M_ν) can be decomposed into $M = P\overline{M}P^T$, where P denotes a diagonal phase matrix and $\overline{M}$ is a real mass matrix with three positive non-vanishing elements. The diagonalization of $\overline{M}$ requires an orthogonal transformation:

$$O^\dagger \overline{M} O^* = \begin{pmatrix} \lambda_1 & 0 & 0 \\ 0 & \lambda_2 & 0 \\ 0 & 0 & \lambda_3 \end{pmatrix} , \tag{16}$$

  where λ_i (for $i = 1, 2, 3$) stand for the physical masses of charged leptons (i.e., $\lambda_{1,2,3} = m_{e,\mu,\tau}$) or neutrinos (i.e., $\lambda_i = m_i$). Then the unitary matrix U (i.e., U_l or U_ν) used to diagonalize M takes the form $U = PO$.

- Note that the matrix elements of $\overline{M}$ and O can be determined in terms of λ_i. This calculability allows us to express the rank-3 (or rank-2) patterns of M in a universal way, as shown in Table II. It turns out that the relation

$$M_{\rm I_n} = E_{\rm n} M_{\rm I_1} E_{\rm n}^T , \quad ({\rm n} = 1, \cdots, 6) \tag{17}$$

  holds for those rank-3 textures, where

[3] If the reported evidence for the existence of the neutrinoless double beta decay [20] is taken into account, one has 0.05 eV $\leq \langle m \rangle_{ee} \leq 0.84$ eV at the 95% confidence level.

$$E_1 = \begin{pmatrix} 1 & 0 & 0 \\ 0 & 1 & 0 \\ 0 & 0 & 1 \end{pmatrix} \; , \quad E_2 = \begin{pmatrix} 1 & 0 & 0 \\ 0 & 0 & 1 \\ 0 & 1 & 0 \end{pmatrix} \; , \quad E_3 = \begin{pmatrix} 0 & 1 & 0 \\ 1 & 0 & 0 \\ 0 & 0 & 1 \end{pmatrix} \; ,$$
$$E_4 = \begin{pmatrix} 0 & 1 & 0 \\ 0 & 0 & 1 \\ 1 & 0 & 0 \end{pmatrix} \; , \quad E_5 = \begin{pmatrix} 0 & 0 & 1 \\ 1 & 0 & 0 \\ 0 & 1 & 0 \end{pmatrix} \; , \quad E_6 = \begin{pmatrix} 0 & 0 & 1 \\ 0 & 1 & 0 \\ 1 & 0 & 0 \end{pmatrix} \; . \tag{18}$$

As for three rank-2 textures, we have

$$M_{\rm I_7} = E_1 M_{\rm I_7} E_1^T \; , \quad M_{\rm I_8} = E_4 M_{\rm I_7} E_4^T \; , \quad M_{\rm I_9} = E_5 M_{\rm I_7} E_5^T \; . \tag{19}$$

It is easy to check that $E_{\rm n}$ is a real orthogonal matrix; i.e., $E_{\rm n} E_{\rm n}^T = E_{\rm n}^T E_{\rm n} = E_1$ holds. In addition, $E_4 = E_2 E_3 = E_3 E_6 = E_6 E_2$ and $E_5 = E_4^T$ hold.

Eqs. (17) and (19) will be useful to demonstrate the isomeric features of a few categories of lepton mass matrices with six texture zeros, as one can see later on.

A. Six Parallel Patterns (rank-3)

We have six parallel patterns of M_l and M_ν,

M_l	$\rm I_1$	$\rm I_2$	$\rm I_3$	$\rm I_4$	$\rm I_5$	$\rm I_6$
M_ν	$\rm I_1$	$\rm I_2$	$\rm I_3$	$\rm I_4$	$\rm I_5$	$\rm I_6$

, (20)

which are compatible with current neutrino oscillation data at the 3σ level. Given $M_{\rm I_1}^{l,\nu}$ being diagonalized by the unitary matrix $U_{l,\nu}$, $M_{\rm I_n}^{l,\nu}$ (for n > 1) can then be diagonalized by $E_{\rm n} U_{l,\nu}$ as a result of Eq. (17). The lepton flavor mixing matrix derived from $M_{\rm I_n}^l$ and $M_{\rm I_n}^\nu$ is found to be identical to $V = U_l^\dagger U_\nu$, which is derived from $M_{\rm I_1}^l$ and $M_{\rm I_1}^\nu$:

$$V_{\rm n} \equiv (E_{\rm n} U_l)^\dagger (E_{\rm n} U_\nu) = U_l^\dagger (E_{\rm n}^T E_{\rm n}) U_\nu = V \; . \tag{21}$$

This simple relation implies that six parallel patterns of M_l and M_ν are *isomeric* – namely, they are structurally different from one another, but their predictions for lepton masses and flavor mixing are exactly the same [22]. It is therefore enough for us to consider only one of the six patterns in the subsequent discussions. With the help of Eq. (16), the moduli of three non-vanishing elements of M_l or M_ν are given by

$$\begin{aligned} A &= \lambda_3 \left(1 - y + xy\right) \; , \\ B &= \lambda_3 \left[\frac{y(1-x)(1-y)(1+xy)}{1-y+xy}\right]^{1/2} \; , \\ C &= \lambda_3 \left(\frac{xy^2}{1-y+xy}\right)^{1/2} \; , \end{aligned} \tag{22}$$

where the subscript "l" or "ν" has been omitted for simplicity. Furthermore, we obtain the matrix elements of O in terms of the mass ratios x and y (see Table II for the definition of a_i, b_i and c_i):

$$
\begin{aligned}
a_1 &= + \left[\frac{1-y}{(1+x)(1-xy)(1-y+xy)}\right]^{1/2} , \\
a_2 &= -i \left[\frac{x(1+xy)}{(1+x)(1+y)(1-y+xy)}\right]^{1/2} , \\
a_3 &= + \left[\frac{xy^3(1-x)}{(1-xy)(1+y)(1-y+xy)}\right]^{1/2} ; \\
b_1 &= + \left[\frac{x(1-y)}{(1+x)(1-xy)}\right]^{1/2} , \\
b_2 &= +i \left[\frac{1+xy}{(1+x)(1+y)}\right]^{1/2} , \\
b_3 &= + \left[\frac{y(1-x)}{(1-xy)(1+y)}\right]^{1/2} ; \\
c_1 &= - \left[\frac{xy(1-x)(1+xy)}{(1+x)(1-xy)(1-y+xy)}\right]^{1/2} , \\
c_2 &= -i \left[\frac{y(1-x)(1-y)}{(1+x)(1+y)(1-y+xy)}\right]^{1/2} , \\
c_3 &= + \left[\frac{(1-y)(1+xy)}{(1-xy)(1+y)(1-y+xy)}\right]^{1/2} . \qquad (23)
\end{aligned}
$$

Note that a_2, b_2 and c_2 are imaginary, and their nontrivial phases arise from a minus sign of the determinant of M(i.e., $\mathrm{Det}(M) = -AC^2 e^{2i\varphi}$). Because of $0 < x_\nu < 1$ extracted from the solar neutrino oscillation data [1], we can obtain $0 < y_\nu < 1$ from Eq. (22) as required by the positiveness of A_ν, B_ν and C_ν [4]. Hence the six isomeric patterns of lepton mass matrices under discussion guarantee a normal neutrino mass spectrum.

Nine elements of the lepton flavor mixing matrix $V = U_l^\dagger U_\nu = O_l^\dagger (P_l^\dagger P_\nu) O_\nu$ can explicitly be written as

$$
V_{pq} \;=\; (a_p^l)^* a_q^\nu e^{i\alpha} + (b_p^l)^* b_q^\nu e^{i\beta} + (c_p^l)^* c_q^\nu \; , \qquad (24)
$$

where the subscripts p and q run respectively over (e, μ, τ) and $(1, 2, 3)$, and the phase parameters α and β are defined by $\alpha \equiv (\varphi_\nu - \varphi_l) - \beta$ and $\beta \equiv (\phi_\nu - \phi_l)$. Note that V consists of four free parameters x_ν, y_ν, α and β. The latter can be constrained, with the help of Eqs. (11) and (12), by using the experimental data listed in Table I ($\Delta m^2_{31} > 0$ as a consequences of $0 < y_\nu < 1$). Once the parameter space of (x_ν, y_ν) and (α, β) is fixed, one may quantitatively determine the Jarlskog invariant $\mathcal{J}$ and three CP-violating phases (δ, ρ, σ). It is also possible to determine the neutrino mass spectrum and two effective

[4] Although $y_\nu > 1$ is in principle allowed by rephasing the non-vanishing elements of M_ν, our numerical analysis indicates that this possibility is actually incompatible with current experimental data.

masses $\langle m \rangle_e$ and $\langle m \rangle_{ee}$ defined in Eq. (15). The results of our numerical calculations are summarized in Figs. 1–3. Some discussions are in order.

1. We have noticed that the parameter space of (x_ν, y_ν) or (α, β) will be empty, if the best-fit values or the 2σ intervals of Δm^2_{21}, Δm^2_{31}, $\sin^2\theta_{12}$, $\sin^2\theta_{23}$ and $\sin^2\theta_{13}$ are taken into account. This situation is due to a potential conflict between the largeness of $\sin^2\theta_{23}$ and the smallness of R_ν, which cannot simultaneously be fulfilled for six parallel patterns of M_l and M_ν at or below the 2σ level.

2. If the 3σ intervals of Δm^2_{21}, Δm^2_{31}, $\sin^2\theta_{12}$, $\sin^2\theta_{23}$ and $\sin^2\theta_{13}$ are used, however, the consequences of M_l and M_ν on two neutrino mass-squared differences and three flavor mixing angles can be compatible with current experimental data. Fig. 1 shows the allowed parameter space of (x_ν, y_ν) and (α, β) at the 3σ level. We see that $\beta \sim \pi$ holds. This result is certainly consistent with the previous observation [14]. Because of $y_\nu \sim 0.25$, $m_3 \approx \sqrt{\Delta m^2_{31}}$ is a good approximation. The neutrino mass spectrum can actually be determined to an acceptable degree of accuracy by using Eq. (13). For instance, we obtain $m_3 \approx (3.8 - 6.1) \times 10^{-2}$ eV, $m_2 \approx (0.95 - 1.5) \times 10^{-2}$ eV and $m_1 \approx (2.6 - 3.4) \times 10^{-3}$ eV, where $x_\nu \approx 1/3$ and $y_\nu \approx 1/4$ have typically been taken.

3. Fig. 2 shows the outputs of $\sin^2\theta_{12}$, $\sin^2\theta_{23}$ and $\sin^2\theta_{13}$ versus R_ν at the 3σ level. One may observe that the maximal atmospheric neutrino mixing (i.e., $\sin^2\theta_{23} \approx 0.5$ or $\sin^2 2\theta_{23} \approx 1$) cannot be achieved from the isomeric lepton mass matrices under consideration. To be specific, $\sin^2\theta_{23} < 0.40$ (or $\sin^2 2\theta_{23} < 0.96$) holds in our ansatz. It is impossible to get a larger value of $\sin^2\theta_{23}$ even if R_ν approaches its upper limit. In contrast, the output of $\sin^2\theta_{12}$ is favorable and has less dependence on R_ν. One may also see that only small values of $\sin^2\theta_{13}$ (≤ 0.016) are favored. More precise experimental data on $\sin^2\theta_{23}$, $\sin^2\theta_{13}$ and R_ν will allow us to examine whether those parallel patterns of lepton mass matrices with six texture zeros can really survive the experimental test or not.

4. Fig. 3 illustrates the results of two effective masses $\langle m \rangle_e$ and $\langle m \rangle_{ee}$, three CP-violating phases (δ, ρ, σ), and the Jarlskog invariant $\mathcal{J}$. It is obvious that $\langle m \rangle_e \sim 10^{-2}$ eV for the tritium beta decay and $\langle m \rangle_{ee} \sim 10^{-3}$ eV for the neutrinoless double beta decay. Both of them are too small to be experimentally accessible in the foreseeable future. We find that the maximal magnitude of $\mathcal{J}$ is close to 0.015 around $\delta \sim 3\pi/4$ (or $5\pi/4$). As for the Majorana phases ρ and σ, the relation $(\rho - \sigma) \approx \pi/2$ holds. This result is attributed to the fact that the matrix elements $(a^\nu_2, b^\nu_2, c^\nu_2)$ of U_ν are all imaginary and they give rise to an irremovable phase shift between V_{p1} and V_{p2} (for $p = e, \mu, \tau$) elements through Eq. (23). Such a phase difference affects $\langle m \rangle_{ee}$, but it has nothing to do with $\langle m \rangle_e$ and $\mathcal{J}$.

To relax the potential tension between the smallness of R_ν and the largeness of $\sin^2\theta_{23}$, we shall incorporate a simple seesaw scenario in the six-zero textures of charged lepton and Dirac neutrino mass matrices in section IV.

B. Six Non-parallel Patterns (rank-3)

The following six non-parallel patterns of M_l and M_ν,

M_l	I_1	I_2	I_3	I_4	I_5	I_6
M_ν	I_2	I_1	I_5	I_6	I_3	I_4

, (25)

in which M_ν is of rank 3, are found to be compatible with current neutrino oscillation data at the 3σ level. Given $M^l_{\mathrm{I}_1}$ and $M^\nu_{\mathrm{I}_2}$ being diagonalized respectively by the unitary matrices U_l and $E_2 U_\nu$, where $U_{l,\nu} = P_{l,\nu} O_{l,\nu}$ with $O_{l,\nu}$ being simple functions of $x_{l,\nu}$ and $y_{l,\nu}$ as already shown in Eq. (23), the corresponding flavor mixing matrix reads

$$V_{pq} \; = \; (a^l_p)^* a^\nu_q e^{i\alpha} + (b^l_p)^* c^\nu_q e^{i\beta} + (c^l_p)^* b^\nu_q \; , \tag{26}$$

where the subscripts p and q run respectively over (e, μ, τ) and $(1, 2, 3)$, the phase parameters α and β are defined by $\alpha \equiv (\varphi_\nu - \varphi_l) - (2\phi_\nu - \phi_l)$ and $\beta \equiv -(\phi_\nu + \phi_l)$, and an overall phase factor $e^{i\phi_\nu}$ has been omitted. Taking account of the other five combinations of M_l and M_ν in Eq. (25), we notice that $M^l_{\mathrm{I}_\mathrm{n}}$ (for $\mathrm{n} \neq 1$) and $M^\nu_{\mathrm{I}_\mathrm{n}}$ (for $\mathrm{n} \neq 2$) can be diagonalized by $E_\mathrm{n} U_l$ and $(E_\mathrm{n} E_2^T) U_\nu$, respectively. Because the relation

$$E_2^T (E_1 E_2^T) = E_3^T (E_5 E_2^T) = E_4^T (E_6 E_2^T) = E_5^T (E_3 E_2^T) = E_6^T (E_4 E_2^T) = E_1 \tag{27}$$

holds, Eq. (26) is universally valid for all six patterns. They are therefore isomeric.

We do a numerical analysis of six non-parallel patterns of M_l and M_ν in Eq. (25). The parameter space of (x_ν, y_ν) or (α, β) is found to be acceptable, when the 3σ intervals of Δm^2_{21}, Δm^2_{31}, $\sin^2\theta_{12}$, $\sin^2\theta_{23}$ and $\sin^2\theta_{13}$ are used. Our explicit results are summarized in Figs. 4–6. Some brief discussions are in order.

1. Fig. 4 shows the allowed parameter space of (x_ν, y_ν) and (α, β) at the 3σ level. We see that $\beta \sim 0$ (or $\beta \sim 2\pi$) holds, while α is essentially unrestricted. Again, $m_3 \approx \sqrt{\Delta m^2_{31}}$ is a good approximation. The neutrino mass spectrum can roughly be determined by using Eq. (13). Note that $x_\nu \sim 0.7$ is marginally allowed – in this case, m_1 and m_2 are approximately of the same order.

2. The outputs of $\sin^2\theta_{12}$, $\sin^2\theta_{23}$ and $\sin^2\theta_{13}$ versus R_ν are illustrated in Fig. 5. We are unable to obtain the maximal atmospheric neutrino mixing (i.e., $\sin^2\theta_{23} \approx 0.5$ or equivalently $\sin^2 2\theta_{23} \approx 1$) from the non-parallel patterns of lepton mass matrices under consideration. Indeed, $\sin^2\theta_{23} > 0.60$ (or $\sin^2 2\theta_{23} < 0.96$) holds in our ansatz. It is impossible to get a larger value of $\sin^2 2\theta_{23}$ even if R_ν approaches its upper bound. In comparison, the output of $\sin^2\theta_{12}$ is favorable and has less dependence on R_ν. Only small values of $\sin^2\theta_{13}$ (≤ 0.02) are allowed.

3. The numerical results for $\langle m \rangle_{ee}/m_3$ versus $\langle m \rangle_e/m_3$, $\mathcal{J}$ versus δ, and σ versus ρ are shown in Fig. 6. Both $\langle m \rangle_e \sim 10^{-2}$ eV and $\langle m \rangle_{ee} \sim 10^{-3}$ eV are too small to be observable. The maximal magnitude of $\mathcal{J}$ is close to 0.02 around $\delta \sim \pm\pi/4$, and the relation $(\sigma - \rho) \approx \pi/2$ holds for two Majorana phases of CP violation.

Comparing the parallel patterns of $M_{l,\nu}$ in Eq. (20) with those non-parallel patterns of $M_{l,\nu}$ in Eq. (25), we find that most of their phenomenological consequences are quite similar. Therefore, it is experimentally difficult to distinguish between them.

C. Twelve Non-parallel Patterns ($m_1 = 0$)

Current neutrino oscillation data cannot exclude the possibility that the neutrino mass m_1 or m_3 vanishes. Hence M_ν is in principle allowed to take the rank-2 textures ($M_{\rm I_7}$, $M_{\rm I_8}$ and $M_{\rm I_9}$) listed in Table II. After a careful analysis, we find that there exist four groups of non-parallel patterns of M_l and M_ν with $m_1 = 0$, which are compatible with the present experimental data at the 3σ level:

M_l	$\rm I_1$	$\rm I_4$	$\rm I_5$
M_ν	$\rm I_7$	$\rm I_8$	$\rm I_9$

, (28a)

M_l	$\rm I_3$	$\rm I_2$	$\rm I_6$
M_ν	$\rm I_7$	$\rm I_8$	$\rm I_9$

, (28b)

M_l	$\rm I_2$	$\rm I_6$	$\rm I_3$
M_ν	$\rm I_7$	$\rm I_8$	$\rm I_9$

, (28c)

M_l	$\rm I_5$	$\rm I_1$	$\rm I_4$
M_ν	$\rm I_7$	$\rm I_8$	$\rm I_9$

. (28d)

The possibility of $m_3 = 0$ has been ruled out. With the help of Eqs. (18) and (19), it is easy to prove that three combinations of M_l and M_ν in each of the above four groups are isomeric. For the charged leptons, the expressions of (A_l, B_l, C_l) and (a_i, b_i, c_i) can be found in Eqs. (22) and (23). As for the neutrinos, we obtain

$$\begin{aligned} \tilde{A}_\nu &= m_3 \left(1 - y_\nu\right) \; , \\ \tilde{B}_\nu &= m_3 \sqrt{y_\nu - z_\nu^2} \; , \end{aligned} \tag{29}$$

where $z_\nu \equiv \tilde{C}_\nu / m_3$. We see that it is impossible to fix $\tilde{C}_\nu$ (or $\tilde{B}_\nu$) in terms of m_i, due to the fact that ${\rm Det}(M_\nu) = 0$ holds. This freedom will be removed, however, once the flavor mixing parameters derived from M_l and M_ν are confronted with the experimental data. To see this point more clearly, we write out the explicit results of nine elements of the lepton flavor mixing matrix V for every group of M_l and M_ν:

$$V_{pq} = (a^l_p)^* \tilde{a}^\nu_q e^{i\alpha} + (b^l_p)^* \tilde{b}^\nu_q e^{i\beta} + (c^l_p)^* \tilde{c}^\nu_q \tag{30a}$$

with $\alpha \equiv \tilde{\phi}_\nu - (\varphi_l - \phi_l)$ and $\beta \equiv \tilde{\varphi}_\nu - \phi_l$ corresponding to Eq. (28a);

$$V_{pq} = (b^l_p)^* \tilde{a}^\nu_q e^{i\alpha} + (a^l_p)^* \tilde{b}^\nu_q e^{i\beta} + (c^l_p)^* \tilde{c}^\nu_q \tag{30b}$$

with $\alpha \equiv \tilde{\phi}_\nu - \phi_l$ and $\beta \equiv \tilde{\varphi}_\nu - (\varphi_l - \phi_l)$ corresponding to Eq. (28b);

$$V_{pq} = (a^l_p)^* \tilde{a}^\nu_q e^{i\alpha} + (c^l_p)^* \tilde{b}^\nu_q e^{i\beta} + (b^l_p)^* \tilde{c}^\nu_q \tag{30c}$$

with $\alpha \equiv \tilde{\phi}_\nu - (\varphi_l - 2\phi_l)$ and $\beta \equiv \tilde{\varphi}_\nu + \phi_l$ corresponding to Eq. (28c); and

$$V_{pq} = (c^l_p)^* \tilde{a}^\nu_q e^{i\alpha} + (a^l_p)^* \tilde{b}^\nu_q e^{i\beta} + (b^l_p)^* \tilde{c}^\nu_q \tag{30d}$$

with $\alpha \equiv \tilde{\phi}_\nu + \phi_l$ and $\beta \equiv \tilde{\varphi}_\nu - (\varphi_l - 2\phi_l)$ corresponding to Eq. (28d), where

$$\begin{aligned}
&\tilde{a}^\nu_1 = -\frac{z_\nu}{\sqrt{y_\nu}} \; , \qquad \tilde{a}^\nu_2 = i\frac{\sqrt{y_\nu - z^2_\nu}}{\sqrt{y_\nu + y^2_\nu}} \; , \qquad \tilde{a}^\nu_3 = \frac{\sqrt{y_\nu - z^2_\nu}}{\sqrt{1 + y_\nu}} \; ; \\
&\tilde{b}^\nu_1 = \frac{\sqrt{y_\nu - z^2_\nu}}{\sqrt{y_\nu}} \; , \qquad \tilde{b}^\nu_2 = i\frac{z_\nu}{\sqrt{y_\nu + y^2_\nu}} \; , \qquad \tilde{b}^\nu_3 = \frac{z_\nu}{\sqrt{1 + y_\nu}} \; ; \\
&\tilde{c}^\nu_1 = 0 \; , \qquad \tilde{c}^\nu_2 = -i\frac{\sqrt{y_\nu}}{\sqrt{1 + y_\nu}} \; , \qquad \tilde{c}^\nu_3 = \frac{1}{\sqrt{1 + y_\nu}} \; .
\end{aligned} \tag{31}$$

In obtaining Eqs. (30c) and (30d), we have omitted an overall phase factor $e^{-i\phi_l}$.

Note that the sum $|\tilde{a}^\nu_i|^2 + |\tilde{b}^\nu_i|^2$ (for $i = 1, 2, 3$) is independent of the free parameter z_ν. This result implies that V_{pq} in Eq. (30b) can be arranged to amount to V_{pq} in Eq. (30a). Indeed, the replacements $z_\nu \Longleftrightarrow \sqrt{y_\nu - z^2_\nu}$ and $\alpha \Longleftrightarrow \beta$ (or equivalently $\tilde{\phi}_\nu \Longleftrightarrow \tilde{\varphi}_\nu$) allow us to transform (V_{p1}, V_{p2}, V_{p3}) of Eq. (30a) into $(-V_{p1}, V_{p2}, V_{p3})$ of Eq. (30b). The extra minus sign of V_{p1} appearing in such a transformation does not make any physical sense, because it can be removed by redefining the phases of three charged lepton fields. Thus we expect that Eqs. (30a) and (30b) lead to identical results for lepton flavor mixing and CP violation. One may show that Eqs. (30c) and (30d) result in the same lepton flavor mixing and CP violation in a similar way. For this reason, it is only needed to numerically analyze the non-parallel patterns of M_l and M_ν in Eqs. (28a) and (28c).

A numerical analysis indicates that the parameter space of (y_ν, z_ν) or (α, β) can be found, if the 3σ intervals of Δm^2_{21}, Δm^2_{31}, $\sin^2\theta_{12}$, $\sin^2\theta_{23}$ and $\sin^2\theta_{13}$ are taken into account. Our results are summarized in Figs. 7–12. Some comments are in order.

1. The parameter space and predictions of M_l and M_ν listed in Eq. (28a) are shown in Figs. 7–9. We see that $\beta \sim \pi$ is favored but $\alpha \sim \pi$ is disfavored. The neutrino mass spectrum has a clear hierarchy: $x_\nu = 0$ and $y_\nu \sim 0.25$. The outputs of $\sin^2\theta_{12}$ and $\sin^2\theta_{23}$ are well constrained, and they seem to favor the corresponding experimental lower bounds. Again, it is impossible to obtain the maximal atmospheric neutrino mixing. We observe that large values of $\sin^2\theta_{13}$, more or less close to its experimental upper limit, are strongly favored. This interesting feature makes the present ansatz experimentally distinguishable from those given in Eqs. (20) and (25). As a straightforward consequence of the normal neutrino mass hierarchy, the results of $\langle m \rangle_e$ and $\langle m \rangle_{ee}$ are both too small to be observable in the near future. The maximal magnitude of $\mathcal{J}$ is close to 0.02 around $|\delta| \sim \pm\pi/7$. As for the Majorana phases, we get the relation $(\sigma - \rho) \approx \pi/2$ (or $-3\pi/2$).

2. The parameter space of M_l and M_ν in Eq. (28b) can be obtained from Fig. 7 with the replacements $z_\nu \Longleftrightarrow \sqrt{y_\nu - z^2_\nu}$ and $\alpha \Longleftrightarrow \beta$. Such replacements are actually equivalent to $\tilde{B}_\nu \Longleftrightarrow \tilde{C}_\nu$ and $\tilde{\phi}_\nu \Longleftrightarrow \tilde{\varphi}_\nu$ between M_ν in Eq. (28a) and its counterpart in Eq. (28b). The phenomenological consequences of M_l and M_ν in both cases are identical, as already shown above.

3. Figs. 10–12 show the allowed parameter space and predictions of M_l and M_ν listed in Eq. (28c). We see that $\alpha \sim \pi$ and $\beta \sim 0$ (or 2π) are essentially favored. The neutrino mass hierarchy is quite similar to that illustrated in Fig. 7. The output of $\sin^2\theta_{23}$ seems to favor the corresponding experimental upper bound, and the maximal atmospheric neutrino mixing cannot be achieved. In comparison, the outputs of $\sin^2\theta_{12}$ and $\sin^2\theta_{13}$ are favorable and have less dependence on R_ν. Note that the predictions of this ansatz for $\langle m\rangle_{ee}$ and $\mathcal{J}$ may reach $0.4m_3$ (at $\langle m\rangle_e \sim 0.15m_3$) and 0.03 (at $\delta \sim \pm 3\pi/4$), respectively. Both results are apparently larger than those obtained above. Again, the relation $(\sigma - \rho) \approx \pi/2$ (or $-3\pi/2$) holds for two Majorana phases.

4. The parameter space of M_l and M_ν in Eq. (28d) can be obtained from Fig. 10 with the replacements $z_\nu \Longleftrightarrow \sqrt{y_\nu - z_\nu^2}$ and $\alpha \Longleftrightarrow \beta$. Their phenomenological consequences are identical to those derived from M_l and M_ν in Eq. (28c).

The main unsatisfactory output of twelve non-parallel patterns of M_l and M_ν, just like the one of six parallel patterns of M_l and M_ν in Eq. (20), is that $\sin^2 2\theta_{23}$ cannot reach the experimentally-favored maximal value. Whether this is really a problem remains to be seen, especially after more accurate neutrino oscillation data are accumulated in the near future.

IV. A SEESAW ANSATZ OF LEPTON MASS MATRICES

To illustrate, let us discuss a simple way to avoid the potential tension between the smallness of R_ν and the largeness of $\sin^2\theta_{23}$ arising from those parallel patterns of M_l and M_ν in Eq. (20). In this connection, we take account of the Fukugita-Tanimoto-Yanagida hypothesis [23] together with the seesaw mechanism [24] – namely, the charged lepton mass matrix M_l and the Dirac neutrino mass matrix $M_{\rm D}$ may take one of the six parallel patterns, while the right-handed Majorana neutrino mass matrix $M_{\rm R}$ takes the form $M_{\rm R} = M_0 E_1$ with M_0 denoting a very large mass scale and E_1 being the unity matrix given in Eq. (18). Then the effective (left-handed) neutrino mass matrix M_ν reads as

$$M_\nu \; = \; M_{\rm D} M_R^{-1} M_{\rm D}^T \; = \; \frac{M_{\rm D}^2}{M_0} \; . \tag{32}$$

For simplicity, we further assume $M_{\rm D}$ to be real (i.e., $\phi_{\rm D} = \varphi_{\rm D} = 0$). It turns out that the real orthogonal transformation $U_{\rm D}$, which is defined to diagonalize $M_{\rm D}$, can simultaneously diagonalize M_ν:

$$U_{\rm D}^T M_\nu U_{\rm D} \; = \; \frac{(U_{\rm D}^T M_{\rm D} U_{\rm D})^2}{M_0} \; = \; \begin{pmatrix} m_1 & 0 & 0 \\ 0 & m_2 & 0 \\ 0 & 0 & m_3 \end{pmatrix} \; , \tag{33}$$

where $m_i \equiv d_i^2/M_0$ with d_i standing for the eigenvalues of $M_{\rm D}$. In terms of the neutrino mass ratios $x_\nu \equiv m_1/m_2 = (d_1/d_2)^2$ and $y_\nu \equiv m_2/m_3 = (d_2/d_3)^2$, we obtain the explicit expressions of nine matrix elements of $U_\nu = U_{\rm D}$:

$$
\begin{aligned}
a^\nu_1 &= + \left[\frac{1-\sqrt{y_\nu}}{(1+\sqrt{x_\nu})(1-\sqrt{x_\nu y_\nu})(1-\sqrt{y_\nu}+\sqrt{x_\nu y_\nu})}\right]^{1/2} , \\
a^\nu_2 &= - \left[\frac{\sqrt{x_\nu}(1+\sqrt{x_\nu y_\nu})}{(1+\sqrt{x_\nu})(1+\sqrt{y_\nu})(1-\sqrt{y_\nu}+\sqrt{x_\nu y_\nu})}\right]^{1/2} , \\
a^\nu_3 &= + \left[\frac{y_\nu\sqrt{x_\nu y_\nu}(1-\sqrt{x_\nu})}{(1-\sqrt{x_\nu y_\nu})(1+\sqrt{y_\nu})(1-\sqrt{y_\nu}+\sqrt{x_\nu y_\nu})}\right]^{1/2} , \\
b^\nu_1 &= + \left[\frac{\sqrt{x_\nu}(1-\sqrt{y_\nu})}{(1+\sqrt{x_\nu})(1-\sqrt{x_\nu y_\nu})}\right]^{1/2} , \\
b^\nu_2 &= + \left[\frac{1+\sqrt{x_\nu y_\nu}}{(1+\sqrt{x_\nu})(1+\sqrt{y_\nu})}\right]^{1/2} , \\
b^\nu_3 &= + \left[\frac{\sqrt{y_\nu}(1-\sqrt{x_\nu})}{(1-\sqrt{x_\nu y_\nu})(1+\sqrt{y_\nu})}\right]^{1/2} , \\
c^\nu_1 &= - \left[\frac{\sqrt{x_\nu y_\nu}(1-\sqrt{x_\nu})(1+\sqrt{x_\nu y_\nu})}{(1+\sqrt{x_\nu})(1-\sqrt{x_\nu y_\nu})(1-\sqrt{y_\nu}+\sqrt{x_\nu y_\nu})}\right]^{1/2} , \\
c^\nu_2 &= - \left[\frac{\sqrt{y_\nu}(1-\sqrt{x_\nu})(1-\sqrt{y_\nu})}{(1+\sqrt{x_\nu})(1+\sqrt{y_\nu})(1-\sqrt{y_\nu}+\sqrt{x_\nu y_\nu})}\right]^{1/2} , \\
c^\nu_3 &= + \left[\frac{(1-\sqrt{y_\nu})(1+\sqrt{x_\nu y_\nu})}{(1-\sqrt{x_\nu y_\nu})(1+\sqrt{y_\nu})(1-\sqrt{y_\nu}+\sqrt{x_\nu y_\nu})}\right]^{1/2} . \qquad (34)
\end{aligned}
$$

The lepton flavor mixing matrix $V = U^\dagger_l U_\nu$ remains to take the same form as Eq. (24), but the relevant phase parameters are now defined as $\alpha \equiv -\varphi_l - \beta$ and $\beta \equiv -\phi_l$. Comparing between Eqs. (23) and (34), one can immediately find that the magnitudes of $(\theta_{12}, \theta_{23}, \theta_{13})$ in the non-seesaw case can be reproduced in the seesaw case with much smaller values of x_ν and y_ν. The latter will allow R_ν to be more strongly suppressed. It is therefore possible to relax the tension between the smallness of R_ν and the largeness of $\sin^2\theta_{23}$ appearing in the non-seesaw case. A careful numerical analysis of six seesaw-modified patterns of lepton mass matrices *does* support this observation. The results of our calculations are summarized as follows.

1. We find that the new ansatz are compatible very well with current neutrino oscillation data, even if the 2σ intervals of Δm^2_{21}, Δm^2_{31}, $\sin^2\theta_{12}$, $\sin^2\theta_{23}$ and $\sin^2\theta_{13}$ are taken into account. Hence it is unnecessary to do a similar analysis at the 3σ level. The parameter space of (x_ν, y_ν) and (α, β) is illustrated in Fig. 13, where $x_\nu \sim y_\nu \sim 0.2$ and $\beta \sim \pi$ hold approximately. Again $m_3 \approx \sqrt{\Delta m^2_{31}}$ is a good approximation. The values of three neutrino masses read explicitly as $m_3 \approx (4.2 - 5.8) \times 10^{-2}$ eV, $m_2 \approx (0.84 - 1.2) \times 10^{-2}$ eV and $m_1 \approx (1.6 - 1.9) \times 10^{-3}$ eV, which are obtained by taking $x_\nu \approx y_\nu \approx 0.2$.

2. The outputs of $\sin^2\theta_{12}$, $\sin^2\theta_{23}$ and $\sin^2\theta_{13}$ versus R_ν are shown in Fig. 14 at the 2σ level. One can see that the magnitude of $\sin^2\theta_{12}$ is essentially unconstrained. Now the maximal atmospheric neutrino mixing (i.e., $\sin^2\theta_{23} \approx 0.5$ or $\sin^2 2\theta_{23} \approx 1$) is achievable in the region of $R_\nu \sim 0.036 - 0.047$. It is also possible to obtain $\sin^2\theta_{13} \leq$

0.035, just below the experimental upper bound [4]. If $\sin^2 2\theta_{13} \geq 0.02$ really holds, the measurement of θ_{13} should be realizable in a future reactor neutrino oscillation experiment [25].

3. Fig. 15 illustrates the numerical results of $\langle m \rangle_e$, $\langle m \rangle_{ee}$, δ, ρ, σ and $\mathcal{J}$. We obtain $\langle m \rangle_e \sim 10^{-2}$ eV for the tritium beta decay and $\langle m \rangle_{ee} \sim 10^{-3}$ eV for the neutrinoless double beta decay – both of them are too small to be experimentally accessible in the near future. We see that $|\mathcal{J}| \sim 0.025$ can be obtained. Such a size of CP violation is expected to be measured in the future long-baseline neutrino oscillation experiments. As for the Majorana phases ρ and σ, the relation $\sigma \approx \rho$ holds. This result is easily understandable, because U_ν is real in the seesaw case. It is worth mentioning that the effective neutrino mass matrix M_ν does not persist in the simple texture as M_l has, thus the allowed ranges of δ, ρ and σ become smaller in the seesaw case than in the non-seesaw case.

It should be noted that the eigenvalues of $M_{\rm D}$ and the heavy Majorana mass scale M_0 are not specified in the above analysis. But one may obtain $|d_1/d_2| = \sqrt{x_\nu} \sim 0.4$ and $|d_2/d_3| = \sqrt{y_\nu} \sim 0.4$. Such a weak hierarchy of $(|d_1|, |d_2|, |d_3|)$ means that $M_{\rm D}$ cannot directly be connected to the charged lepton mass matrix M_l, nor can it be related to the up-type quark mass matrix ($M_{\rm u}$) or its down-type counterpart ($M_{\rm d}$) in a simple way. If the hypothesis $M_{\rm R} = M_0 E_1$ is rejected but the result $U_\nu^T M_\nu U_\nu = {\rm Diag}\{m_1, m_2, m_3\}$ with U_ν given by Eq. (34) is maintained, it will be possible to determine the pattern of $M_{\rm R}$ by means of the inverted seesaw formula $M_{\rm R} = M_{\rm D}^T M_\nu^{-1} M_{\rm D}$ [26] and by assuming a specific relation between $M_{\rm D}$ and $M_{\rm u}$. For example, one may simply assume $M_{\rm D} = M_{\rm u}$ with $M_{\rm u}$ taking the approximate Fritzsch form,

$$M_{\rm u} \sim \begin{pmatrix} {\bf 0} & \sqrt{m_u m_c} & {\bf 0} \\ \sqrt{m_u m_c} & {\bf 0} & \sqrt{m_c m_t} \\ {\bf 0} & \sqrt{m_c m_t} & m_t \end{pmatrix} . \tag{35}$$

Just for the purpose of illustration, we typically input $x_\nu \sim y_\nu \sim 0.18$ as well as $m_u/m_c \sim m_c/m_t \sim 0.0031$ and $m_t \approx 175$ GeV at the electroweak scale [6]. Then we arrive at

$$M_{\rm R} \sim 3.0 \times 10^{15} \times \begin{pmatrix} 6.1 \times 10^{-8} & 1.2 \times 10^{-5} & 2.0 \times 10^{-4} \\ 1.2 \times 10^{-5} & 3.5 \times 10^{-3} & 5.9 \times 10^{-2} \\ 2.0 \times 10^{-4} & 5.9 \times 10^{-2} & {\bf 1} \end{pmatrix} \tag{36}$$

in unit of GeV. This order-of-magnitude estimate shows that the scale of $M_{\rm R}$ is close to that of grand unified theories $\Lambda_{\rm GUT} \sim 10^{16}$ GeV, but the texture of $M_{\rm R}$ and that of $M_{\rm D}$ (or M_l) have little similarity. It is certainly a very nontrivial task to combine the seesaw mechanism and those phenomenologically-favored patterns of lepton mass matrices. In this sense, the simple scenarios discussed in Refs. [22,23] and in the present paper may serve as a helpful example to give readers a ball-park feeling of the problem itself and possible solutions to it.

Of course, a similar application of the seesaw mechanism to the non-parallel patterns of lepton mass matrices is straightforward. In this case, an enhancement of $\sin^2 2\theta_{23}$ up to its maximal value can also be achieved.

V. SUMMARY

To summarize, we have analyzed 400 combinations of the charged lepton and neutrino mass matrices with six texture zeros in a systematic way. Only 24 of them, including 6 parallel patterns and 18 non-parallel patterns, are found to be compatible with current neutrino oscillation data at the 3σ level. Those viable patterns of lepton mass matrices can be classified into a few distinct categories. The textures in each category are demonstrated to have the same phenomenological consequences, such as the normal neutrino mass hierarchy and the bi-large flavor mixing pattern. We have also discussed a very simple way to incorporate the seesaw mechanism in the charged lepton and Dirac neutrino mass matrices with six texture zeros. We illustrate that there is no problem to fit current experimental data even at the 2σ level in the seesaw case. In particular, the maximal atmospheric neutrino mixing can naturally be reconciled with a relatively strong neutrino mass hierarchy. Our results for effective masses of the tritium beta decay and the neutrinoless double beta decay are too small to be experimentally accessible in both the seesaw and non-seesaw cases, but the strength of CP violation can reach the percent level and might be detectable in the upcoming long-baseline neutrino oscillation experiments.

We conclude that the peculiar feature of isomeric lepton mass matrices with six texture zeros is very suggestive for model building. We therefore look forward to seeing whether such simple phenomenological ansätze can survive the more stringent experimental test or not in the near future.

This work was supported in part by the National Natural Science Foundation of China.

REFERENCES

[1] SNO Collaboration, Q.R. Ahmad *et al.*, Phys. Rev. Lett. **87**, 071301 (2001); **89**, 011301 (2002); **89**, 011302 (2002).

[2] Super-Kamiokande Collaboration, Y. Fukuda *et al.*, Phys. Lett. B **467**, 185 (1999); S. Fukuda *et al.*, Phys. Rev. Lett. **85**, 3999 (2000); Phys. Rev. Lett. **86**, 5651 (2001); Phys. Rev. Lett. **86**, 5656 (2001).

[3] KamLAND Collaboration, K. Eguchi *et al.*, Phys. Rev. Lett. **90**, 021802 (2003).

[4] CHOOZ Collaboration, M. Apollonio *et al.*, Phys. Lett. B **420**, 397 (1998); Palo Verde Collaboration, F. Boehm *et al.*, Phys. Rev. Lett. **84**, 3764 (2000).

[5] K2K Collaboration, M.H. Ahn *et al.*, Phys. Rev. Lett. **90**, 041801 (2003).

[6] Particle Data Group, K. Hagiwara *et al.*, Phys. Rev. D **66**, 010001 (2002).

[7] See, e.g., J.N. Bahcall and C. Peña-Garay, JHEP **0311**, 004 (2003); M.C. Gonzalez-Garcia and C. Peña-Garay, Phys. Rev. D **68**, 093003 (2003); M. Maltoni, T. Schwetz, M.A. Tórtola, and J.W.F. Valle, hep-ph/0309130; P.V. de Holanda and A.Yu. Smirnov, hep-ph/0309299; and references therein.

[8] For recent reviews with extensive references, see: H. Fritzsch and Z.Z. Xing, Prog. Part. Nucl. Phys. **45**, 1 (2000); G. Altarelli and F. Feruglio, in *Neutrino Mass* - Springer Tracts in Modern Physics, edited by G. Altarelli and K. Winter (2002) p. 169; S.F. King, Rept. Prog. Phys. **67**, 107 (2004); Z.Z. Xing, Int. J. Mod. Phys. A **19**, 1 (2004).

[9] See, e.g., M. Fukugita, M. Tanimoto, and T. Yanagida, Prog. Theor. Phys. **89**, 263 (1993); Y. Achiman and T. Greiner, Phys. Lett. B **329**, 33 (1994); H. Nishiura, K. Matsuda, and T. Fukuyama, Phys. Rev. D **60**, 013006 (1999); W. Buchmüller and D. Wyler, Phys. Lett. B **521**, 291 (2001); K. Matsuda, Y. Koide, T. Fukuyama, and H. Nishiura, Phys. Rev. D **65**, 033008 (2002); M. Bando and M. Obara, Prog. Theor. Phys. **109**, 995 (2003); M. Bando, S. Kaneko, M. Obara, and M. Tanimoto, hep-ph/0405071. For a recent review with more extensive references, see: M.C. Chen and K.T. Mahanthappa, Int. J. Mod. Phys. A **18**, 5819 (2003).

[10] A. Zee, Phys. Lett. B **93**, 389 (1980).

[11] H. Fritzsch, Phys. Lett. B **73**, 317 (1978); Nucl. Phys. B **155**, 189 (1979).

[12] P. Ramond, R.G. Roberts, and G.G. Ross, Nucl. Phys. B **406**, 19 (1993); H. Fritzsch and Z.Z. Xing, Nucl. Phys. B **556**, 49 (1999).

[13] See, e.g., P.H. Frampton, S.L. Glashow, and D. Marfatia, Phys. Lett. B **536**, 79 (2002); X.G. He, hep-ph/0307172; and references therein.

[14] Z.Z. Xing, Phys. Lett. B **550**, 178 (2002).

[15] To be specific, we make use of the 2σ and 3σ intervals of two neutrino mass-squared differences and three lepton flavor mixing angles given by M. Maltoni *et al* in Ref. [7].

[16] C. Jarlskog, Phys. Rev. Lett. **55**, 1039 (1985).

[17] See, e.g., A. Blondel *et al.*, Nucl. Instrum. Meth. A **451**, 102 (2000); C. Albright *et al.*, hep-ex/0008064; G. Barenboim *et al.*, hep-ex/0304017.

[18] V. Aseev *et al.*, talks given at the International Workshop on Neutrino Masses in the Sub-eV Ranges, Bad Liebenzell, Germany, January 2001; Homepage: http://www-ikl.fzk.de/tritium.

[19] Heidelberg-Moscow Collaboration, H.V. Klapdor-Kleingrothaus, hep-ph/0103074; C.E. Aalseth *et al.*, hep-ex/0202026.

[20] H.V. Klapdor-Kleingrothaus, A. Dietz, H.L. Harney, and I.V. Krivosheina, Mod. Phys. Lett. A **16**, 2409 (2002).
[21] O. Cremonesi, hep-ph/0210007; and references therein.
[22] Z.Z. Xing and S. Zhou, Phys. Lett. B **593**, 156 (2004).
[23] M. Fukugita, M. Tanimoto, and T. Yanagida, Phys. Lett. B **562**, 273 (2003).
[24] T. Yanagida, in *Proceedings of the Workshop on Unified Theory and the Baryon Number of the Universe*, edited by O. Sawada and A. Sugamoto (KEK, Tsukuba, 1979), p. 95; M. Gell-Mann, P. Ramond, and R. Slansky, in *Supergravity*, edited by F. van Nieuwenhuizen and D. Freedman (North Holland, Amsterdam, 1979), p. 315; S.L. Glashow, in *Quarks and Leptons*, edited by M. Lévy *et al.* (Plenum, New York, 1980), p. 707; R.N. Mohapatra and G. Senjanovic, Phys. Rev. Lett. **44**, 912 (1980).
[25] K. Anderson *et al.*, hep-ex/0402041.
[26] Z.Z. Xing and H. Zhang, Phys. Lett. B **569**, 30 (2003).

TABLES

TABLE I. The best-fit values, 2σ and 3σ intervals of Δm^2_{21}, $|\Delta m^2_{31}|$, $\sin^2\theta_{12}$, $\sin^2\theta_{23}$ and $\sin^2\theta_{13}$ obtained from a global analysis of the latest solar, atmospheric, reactor and accelerator neutrino oscillation data [14].

	Δm^2_{21} (10^{-5} eV^2)	$\lvert\Delta m^2_{31}\rvert$ (10^{-3} eV^2)	$\sin^2\theta_{12}$	$\sin^2\theta_{23}$	$\sin^2\theta_{13}$
Best fit	6.9	2.6	0.30	0.52	0.006
2σ	6.0–8.4	1.8–3.3	0.25–0.36	0.36–0.67	≤ 0.035
3σ	5.4–9.5	1.4–3.7	0.23–0.39	0.31–0.72	≤ 0.054

TABLE II. The type-I textures of a symmetric lepton mass matrix M (i.e., M_l or M_ν) and the corresponding forms of the phase matrix P (i.e., P_l or P_ν) and the unitary matrix O (i.e., O_l or O_ν) used to diagonalize M, in which (A, B, C) or $(\tilde{A}, \tilde{B}, \tilde{C})$ are defined to be real and positive.

Rank 3	The mass matrix M	The phase matrix P	The unitary matrix O
I_1	$\begin{pmatrix} \mathbf{0} & Ce^{i\varphi} & \mathbf{0} \\ Ce^{i\varphi} & \mathbf{0} & Be^{i\phi} \\ \mathbf{0} & Be^{i\phi} & A \end{pmatrix}$	$\begin{pmatrix} e^{i(\varphi-\phi)} & 0 & 0 \\ 0 & e^{i\phi} & 0 \\ 0 & 0 & 1 \end{pmatrix}$	$\begin{pmatrix} a_1 & a_2 & a_3 \\ b_1 & b_2 & b_3 \\ c_1 & c_2 & c_3 \end{pmatrix}$
I_2	$\begin{pmatrix} \mathbf{0} & \mathbf{0} & Ce^{i\varphi} \\ \mathbf{0} & A & Be^{i\phi} \\ Ce^{i\varphi} & Be^{i\phi} & \mathbf{0} \end{pmatrix}$	$\begin{pmatrix} e^{i(\varphi-\phi)} & 0 & 0 \\ 0 & 1 & 0 \\ 0 & 0 & e^{i\phi} \end{pmatrix}$	$\begin{pmatrix} a_1 & a_2 & a_3 \\ c_1 & c_2 & c_3 \\ b_1 & b_2 & b_3 \end{pmatrix}$
I_3	$\begin{pmatrix} \mathbf{0} & Ce^{i\varphi} & Be^{i\phi} \\ Ce^{i\varphi} & \mathbf{0} & \mathbf{0} \\ Be^{i\phi} & \mathbf{0} & A \end{pmatrix}$	$\begin{pmatrix} e^{i\phi} & 0 & 0 \\ 0 & e^{i(\varphi-\phi)} & 0 \\ 0 & 0 & 1 \end{pmatrix}$	$\begin{pmatrix} b_1 & b_2 & b_3 \\ a_1 & a_2 & a_3 \\ c_1 & c_2 & c_3 \end{pmatrix}$
I_4	$\begin{pmatrix} \mathbf{0} & Be^{i\phi} & Ce^{i\varphi} \\ Be^{i\phi} & A & \mathbf{0} \\ Ce^{i\varphi} & \mathbf{0} & \mathbf{0} \end{pmatrix}$	$\begin{pmatrix} e^{i\phi} & 0 & 0 \\ 0 & 1 & 0 \\ 0 & 0 & e^{i(\varphi-\phi)} \end{pmatrix}$	$\begin{pmatrix} b_1 & b_2 & b_3 \\ c_1 & c_2 & c_3 \\ a_1 & a_2 & a_3 \end{pmatrix}$
I_5	$\begin{pmatrix} A & \mathbf{0} & Be^{i\phi} \\ \mathbf{0} & \mathbf{0} & Ce^{i\varphi} \\ Be^{i\phi} & Ce^{i\varphi} & \mathbf{0} \end{pmatrix}$	$\begin{pmatrix} 1 & 0 & 0 \\ 0 & e^{i(\varphi-\phi)} & 0 \\ 0 & 0 & e^{i\phi} \end{pmatrix}$	$\begin{pmatrix} c_1 & c_2 & c_3 \\ a_1 & a_2 & a_3 \\ b_1 & b_2 & b_3 \end{pmatrix}$
I_6	$\begin{pmatrix} A & Be^{i\phi} & \mathbf{0} \\ Be^{i\phi} & \mathbf{0} & Ce^{i\varphi} \\ \mathbf{0} & Ce^{i\varphi} & \mathbf{0} \end{pmatrix}$	$\begin{pmatrix} 1 & 0 & 0 \\ 0 & e^{i\phi} & 0 \\ 0 & 0 & e^{i(\varphi-\phi)} \end{pmatrix}$	$\begin{pmatrix} c_1 & c_2 & c_3 \\ b_1 & b_2 & b_3 \\ a_1 & a_2 & a_3 \end{pmatrix}$
Rank 2	The mass matrix M	The phase matrix P	The unitary matrix O
I_7	$\begin{pmatrix} \mathbf{0} & \mathbf{0} & \tilde{B}e^{i\tilde{\phi}} \\ \mathbf{0} & \mathbf{0} & \tilde{C}e^{i\tilde{\varphi}} \\ \tilde{B}e^{i\tilde{\phi}} & \tilde{C}e^{i\tilde{\varphi}} & \tilde{A} \end{pmatrix}$	$\begin{pmatrix} e^{i\tilde{\phi}} & 0 & 0 \\ 0 & e^{i\tilde{\varphi}} & 0 \\ 0 & 0 & 1 \end{pmatrix}$	$\begin{pmatrix} \tilde{a}_1 & \tilde{a}_2 & \tilde{a}_3 \\ \tilde{b}_1 & \tilde{b}_2 & \tilde{b}_3 \\ \tilde{c}_1 & \tilde{c}_2 & \tilde{c}_3 \end{pmatrix}$
I_8	$\begin{pmatrix} \mathbf{0} & \tilde{C}e^{i\tilde{\varphi}} & \mathbf{0} \\ \tilde{C}e^{i\tilde{\varphi}} & \tilde{A} & \tilde{B}e^{i\tilde{\phi}} \\ \mathbf{0} & \tilde{B}e^{i\tilde{\phi}} & \mathbf{0} \end{pmatrix}$	$\begin{pmatrix} e^{i\tilde{\varphi}} & 0 & 0 \\ 0 & 1 & 0 \\ 0 & 0 & e^{i\tilde{\phi}} \end{pmatrix}$	$\begin{pmatrix} \tilde{b}_1 & \tilde{b}_2 & \tilde{b}_3 \\ \tilde{c}_1 & \tilde{c}_2 & \tilde{c}_3 \\ \tilde{a}_1 & \tilde{a}_2 & \tilde{a}_3 \end{pmatrix}$
I_9	$\begin{pmatrix} \tilde{A} & \tilde{B}e^{i\tilde{\phi}} & \tilde{C}e^{i\tilde{\varphi}} \\ \tilde{B}e^{i\tilde{\phi}} & \mathbf{0} & \mathbf{0} \\ \tilde{C}e^{i\tilde{\varphi}} & \mathbf{0} & \mathbf{0} \end{pmatrix}$	$\begin{pmatrix} 1 & 0 & 0 \\ 0 & e^{i\tilde{\phi}} & 0 \\ 0 & 0 & e^{i\tilde{\varphi}} \end{pmatrix}$	$\begin{pmatrix} \tilde{c}_1 & \tilde{c}_2 & \tilde{c}_3 \\ \tilde{a}_1 & \tilde{a}_2 & \tilde{a}_3 \\ \tilde{b}_1 & \tilde{b}_2 & \tilde{b}_3 \end{pmatrix}$

FIGURES

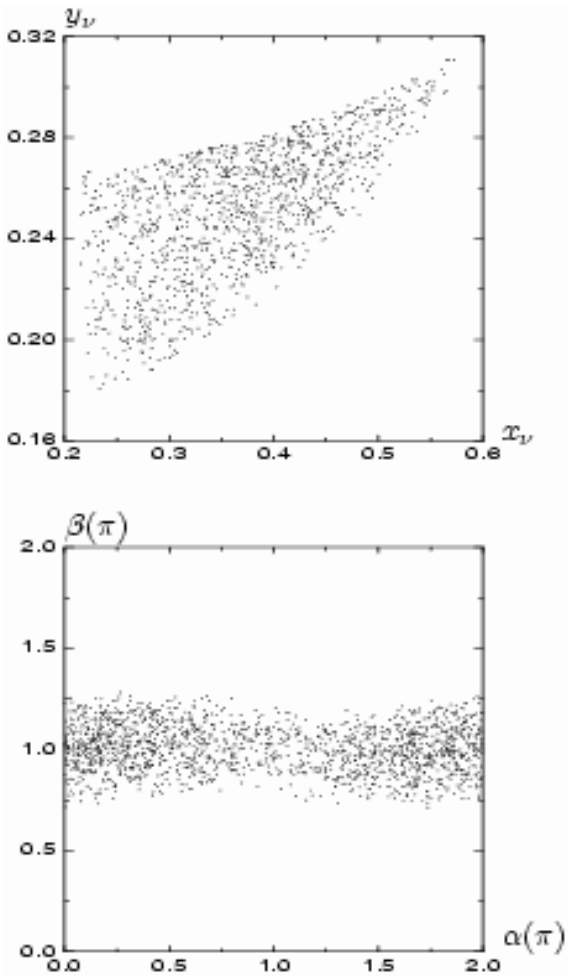

FIG. 1. Parallel patterns of M_l and M_ν in Eq. (20): the parameter space of (x_ν, y_ν) and (α, β) at the 3σ level.

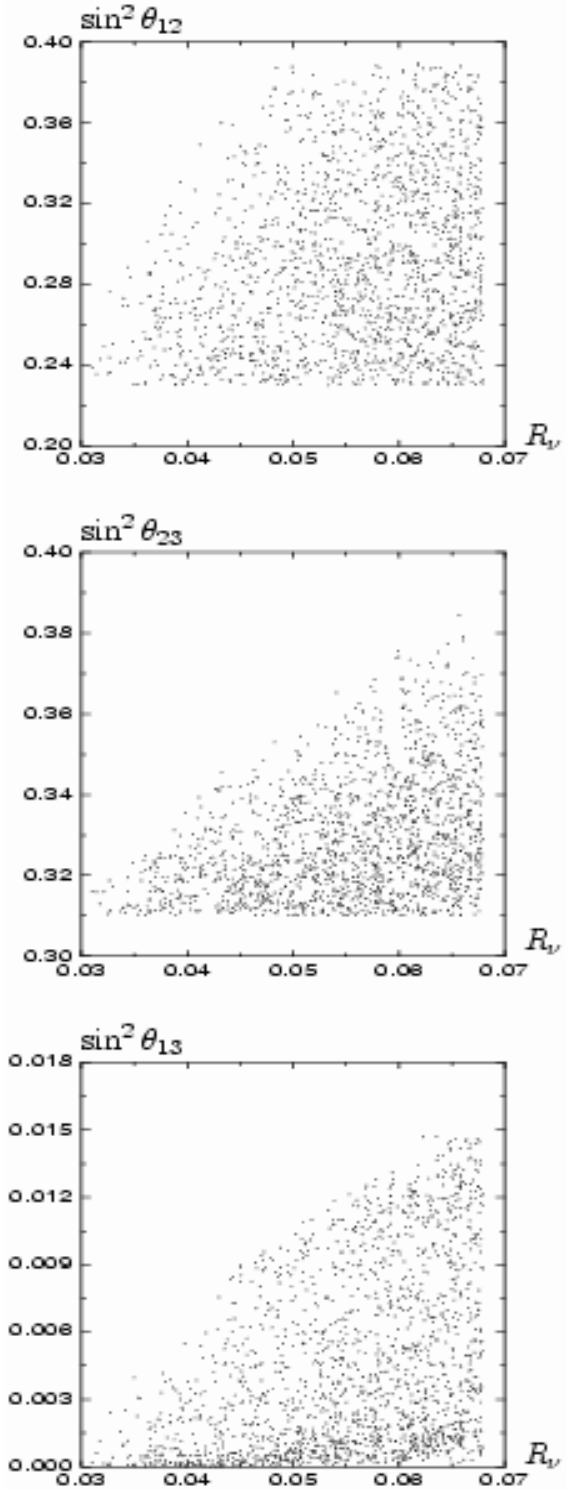

FIG. 2. Parallel patterns of M_l and M_ν in Eq. (20): the outputs of $\sin^2\theta_{12}$, $\sin^2\theta_{23}$ and $\sin^2\theta_{13}$ versus R_ν at the 3σ level.

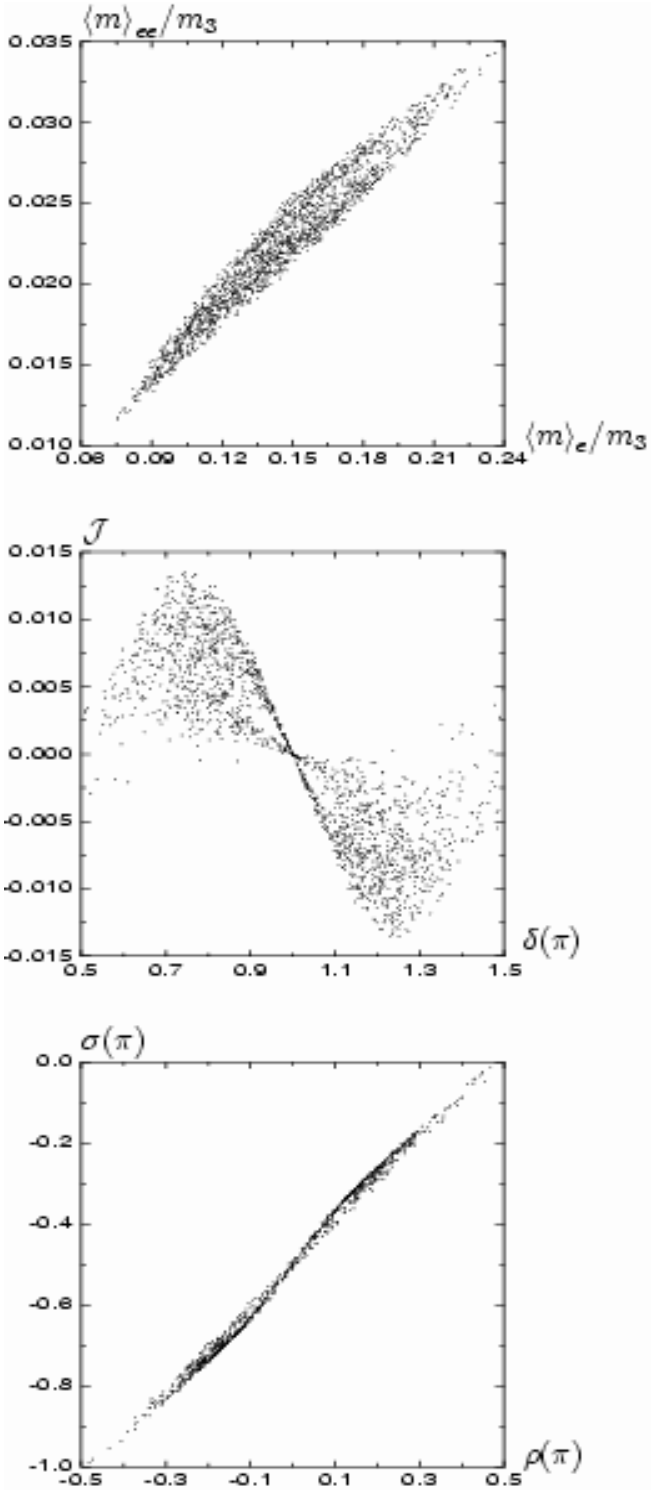

FIG. 3. Parallel patterns of M_l and M_ν in Eq. (20): the outputs of $(\langle m\rangle_e, \langle m\rangle_{ee})$, $(\delta, \mathcal{J})$ and (ρ, σ) at the 3σ level.

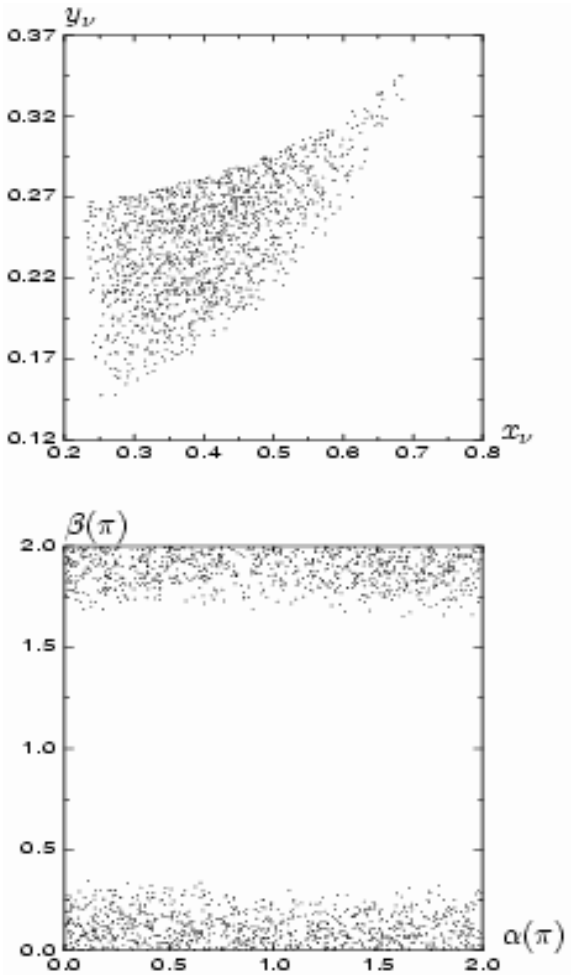

FIG. 4. Non-parallel patterns of M_l and M_ν in Eq. (25): the parameter space of (x_ν, y_ν) and (α, β) at the 3σ level.

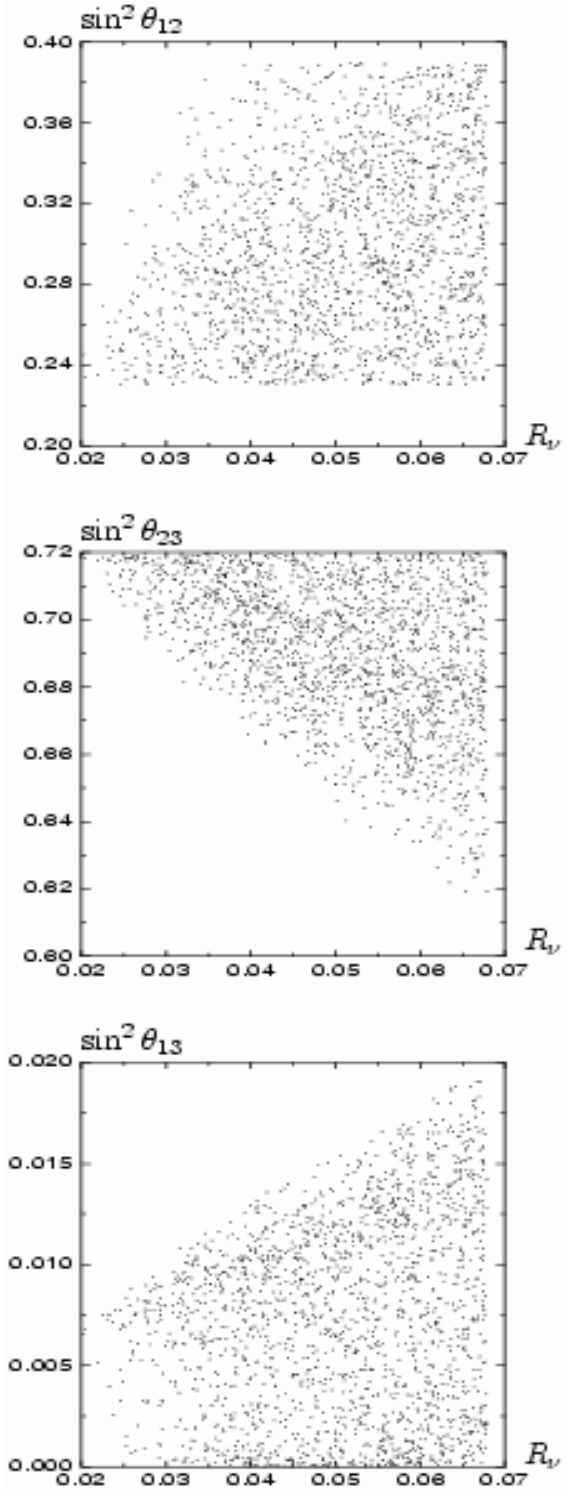

FIG. 5. Non-parallel patterns of M_l and M_ν in Eq. (25): the outputs of $\sin^2\theta_{12}$, $\sin^2\theta_{23}$ and $\sin^2\theta_{13}$ versus R_ν at the 3σ level.

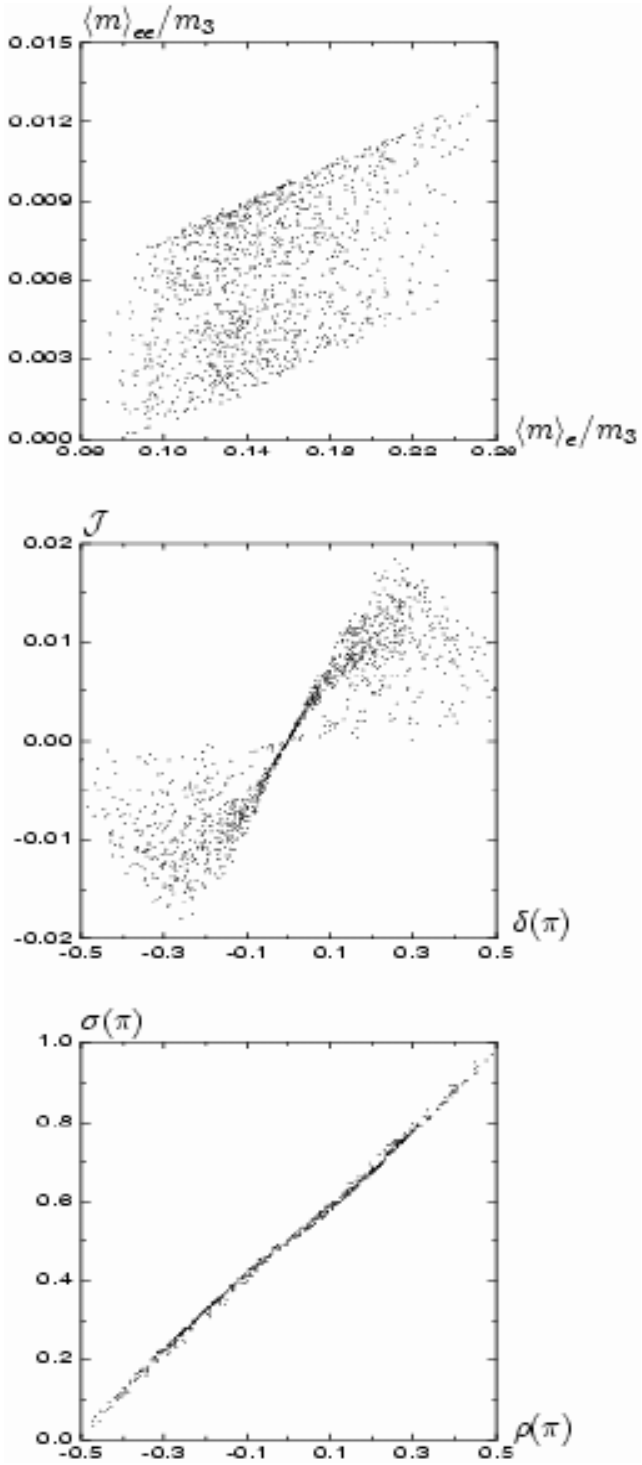

FIG. 6. Non-parallel patterns of M_l and M_ν in Eq. (25): the outputs of $(\langle m\rangle_e, \langle m\rangle_{ee})$, $(\delta, \mathcal{J})$ and (ρ, σ) at the 3σ level.

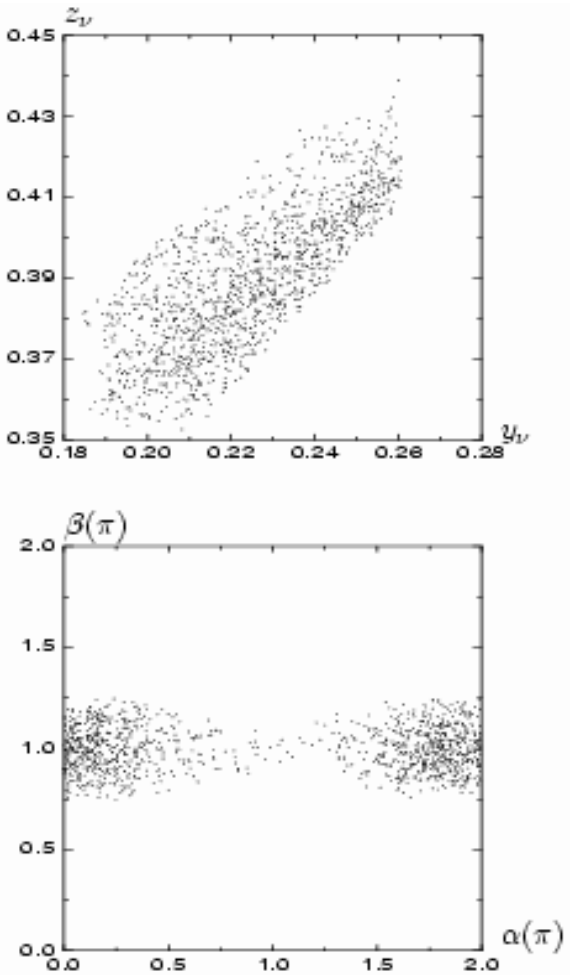

FIG. 7. Non-parallel patterns of M_l and M_ν in Eq. (28a): the parameter space of (y_ν, z_ν) and (α, β) at the 3σ level.

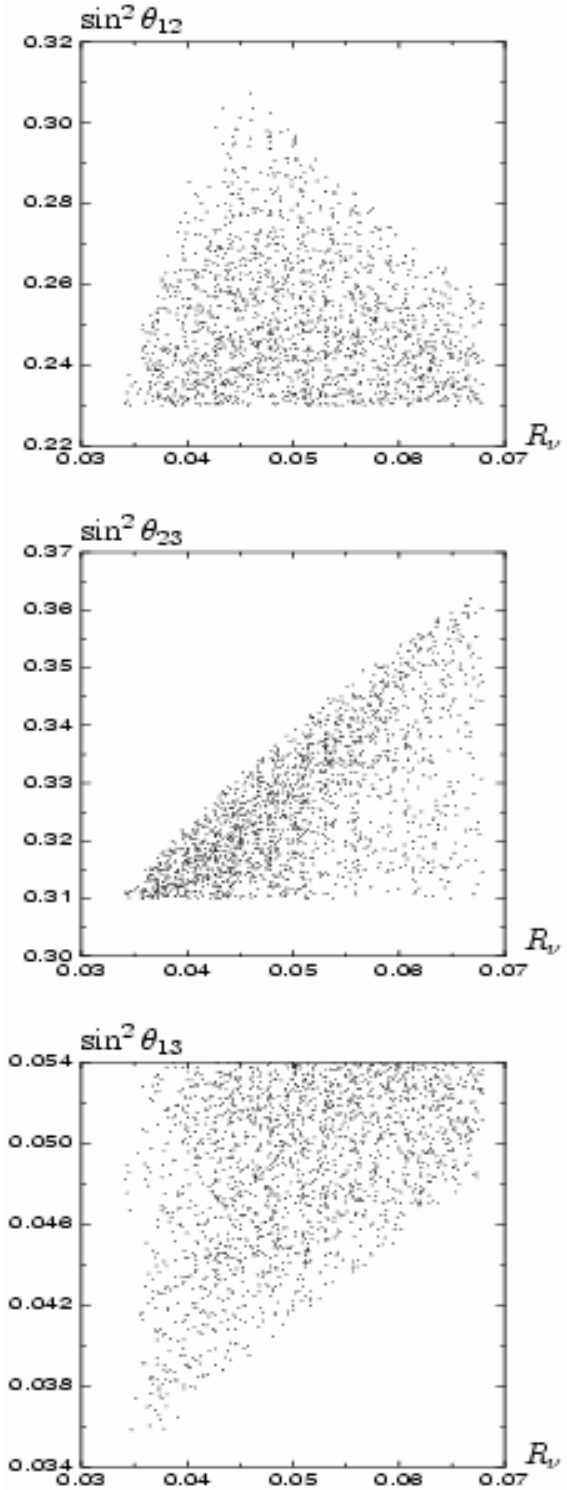

FIG. 8. Non-parallel patterns of M_l and M_ν in Eq. (28a): the outputs of $\sin^2\theta_{12}$, $\sin^2\theta_{23}$ and $\sin^2\theta_{13}$ versus R_ν at the 3σ level.

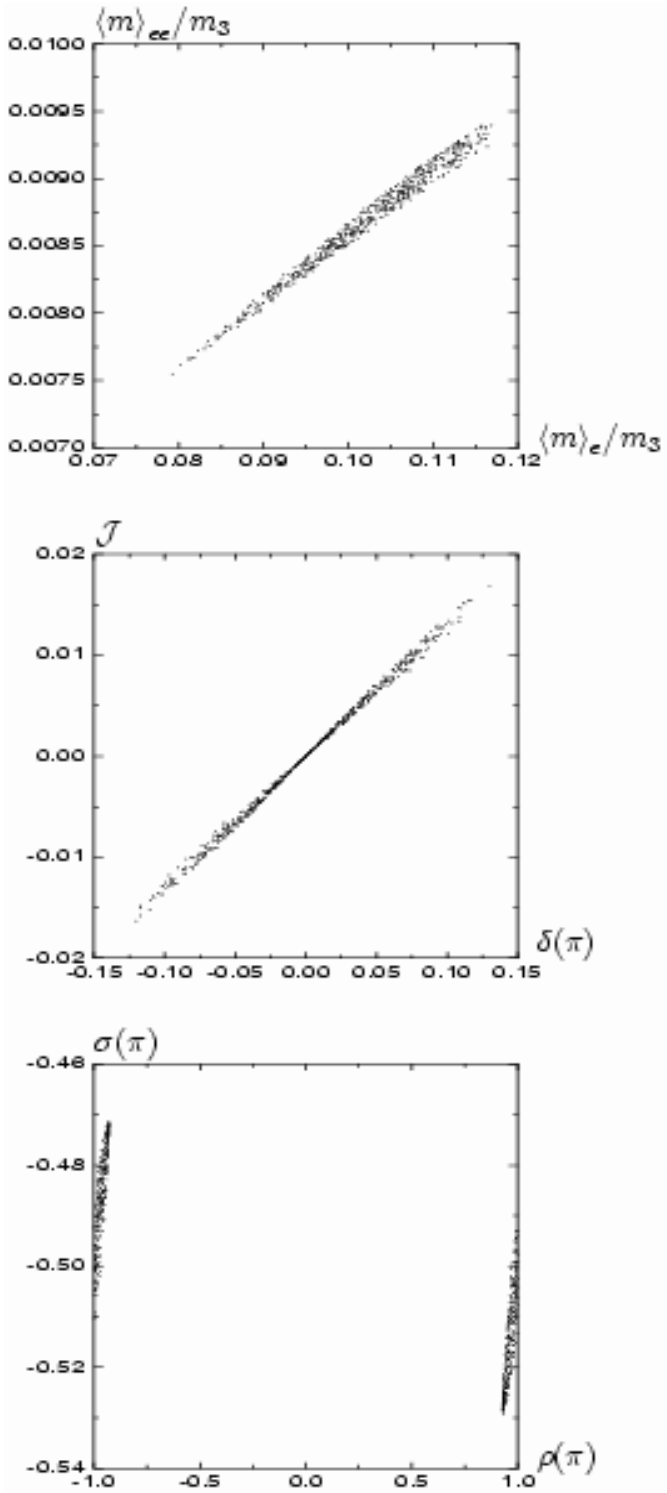

FIG. 9. Non-parallel patterns of M_l and M_ν in Eq. (28a): the outputs of $(\langle m\rangle_e, \langle m\rangle_{ee})$, $(\delta, \mathcal{J})$ and (ρ, σ) at the 3σ level.

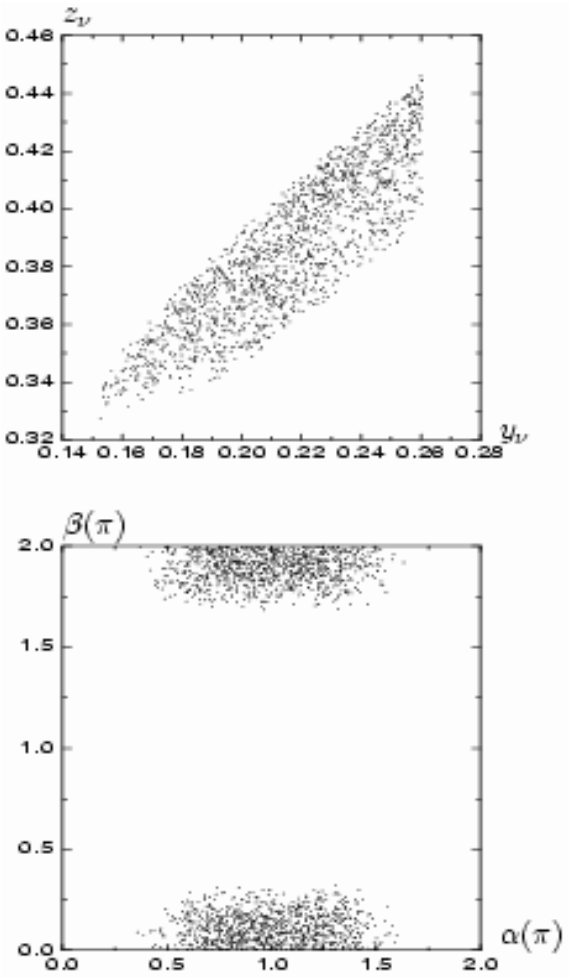

FIG. 10. Non-parallel patterns of M_l and M_ν in Eq. (28c): the parameter space of (y_ν, z_ν) and (α, β) at the 3σ level.

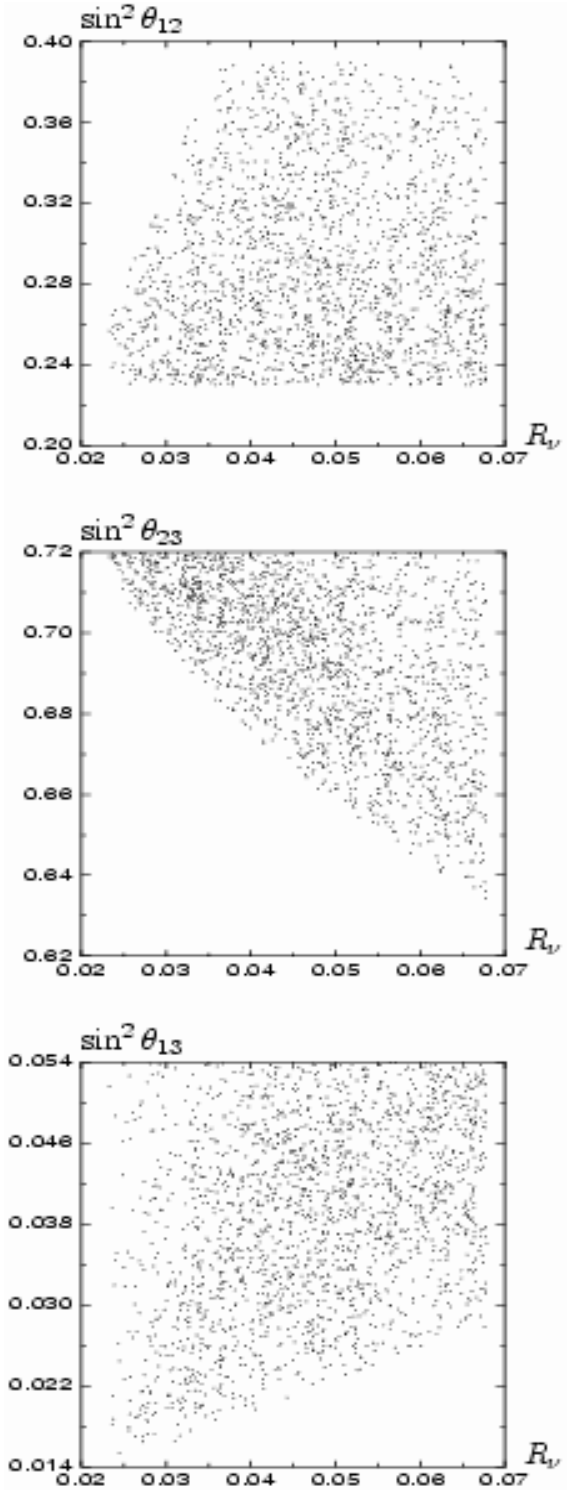

FIG. 11. Non-parallel patterns of M_l and M_ν in Eq. (28c): the outputs of $\sin^2\theta_{12}$, $\sin^2\theta_{23}$ and $\sin^2\theta_{13}$ versus R_ν at the 3σ level.

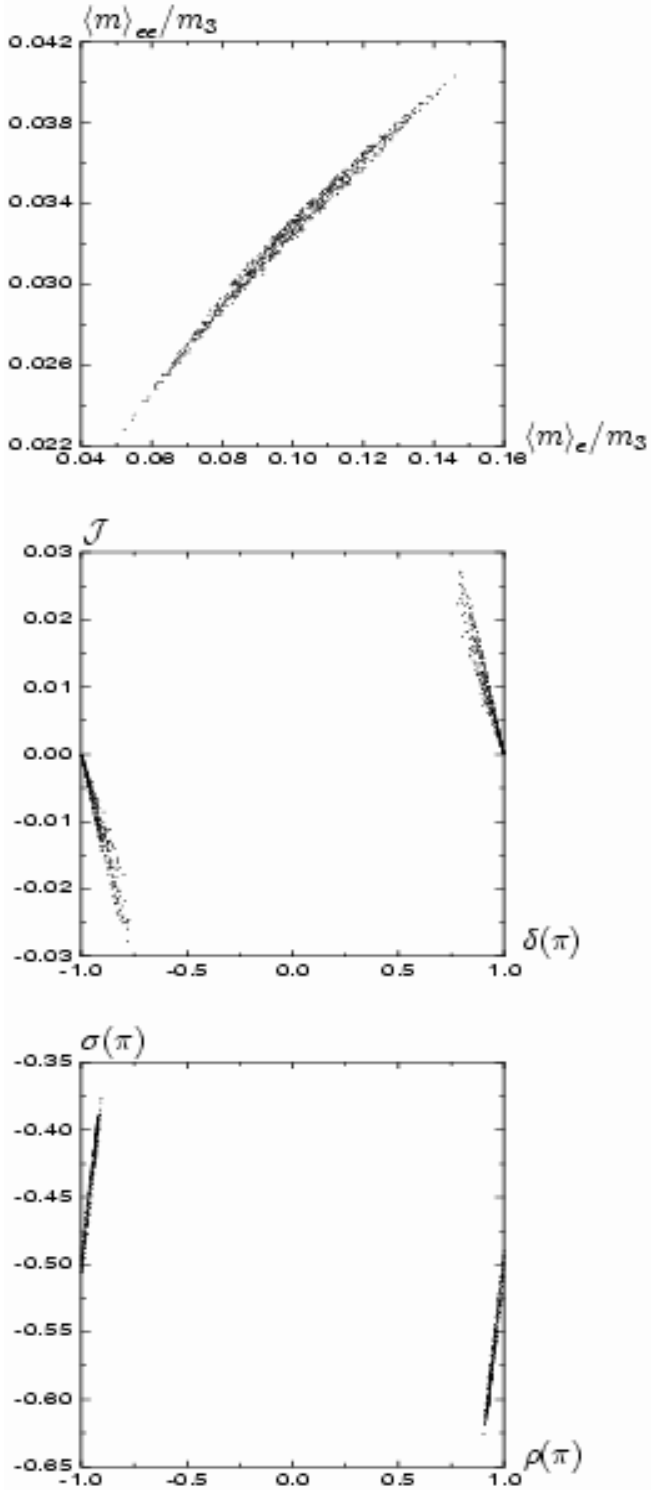

FIG. 12. Non-parallel patterns of M_l and M_ν in Eq. (28c): the outputs of $(\langle m\rangle_e, \langle m\rangle_{ee})$, $(\delta, \mathcal{J})$ and (ρ, σ) at the 3σ level.

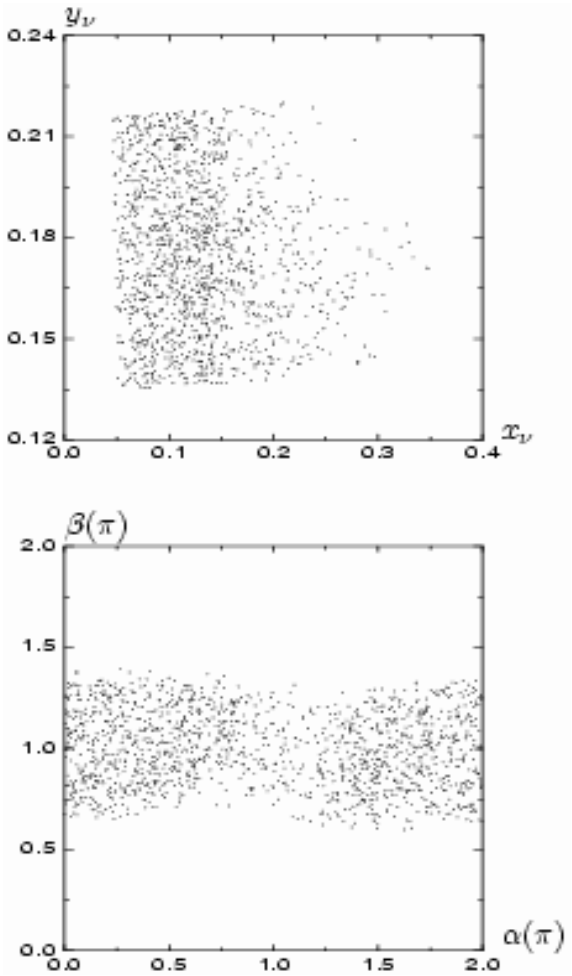

FIG. 13. A simple seesaw example: the parameter space of (x_ν, y_ν) and (α, β) at the 2σ level.

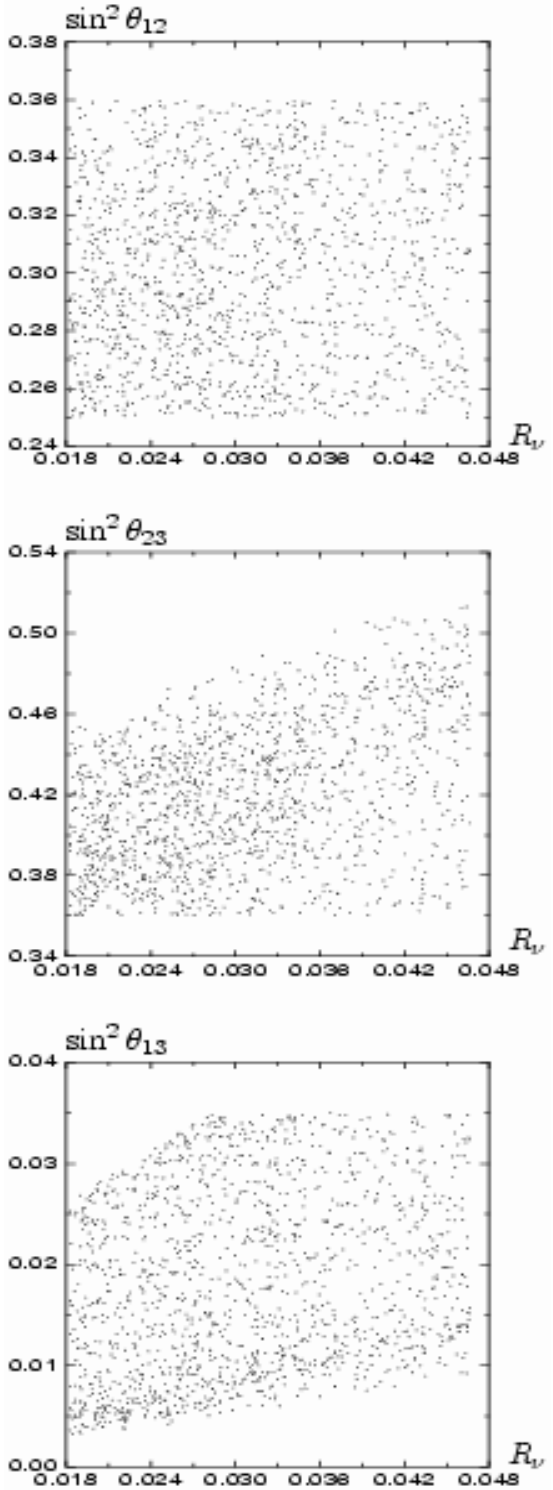

FIG. 14. A simple seesaw example: the outputs of $\sin^2\theta_{12}$, $\sin^2\theta_{23}$ and $\sin^2\theta_{13}$ versus R_ν at the 2σ level.

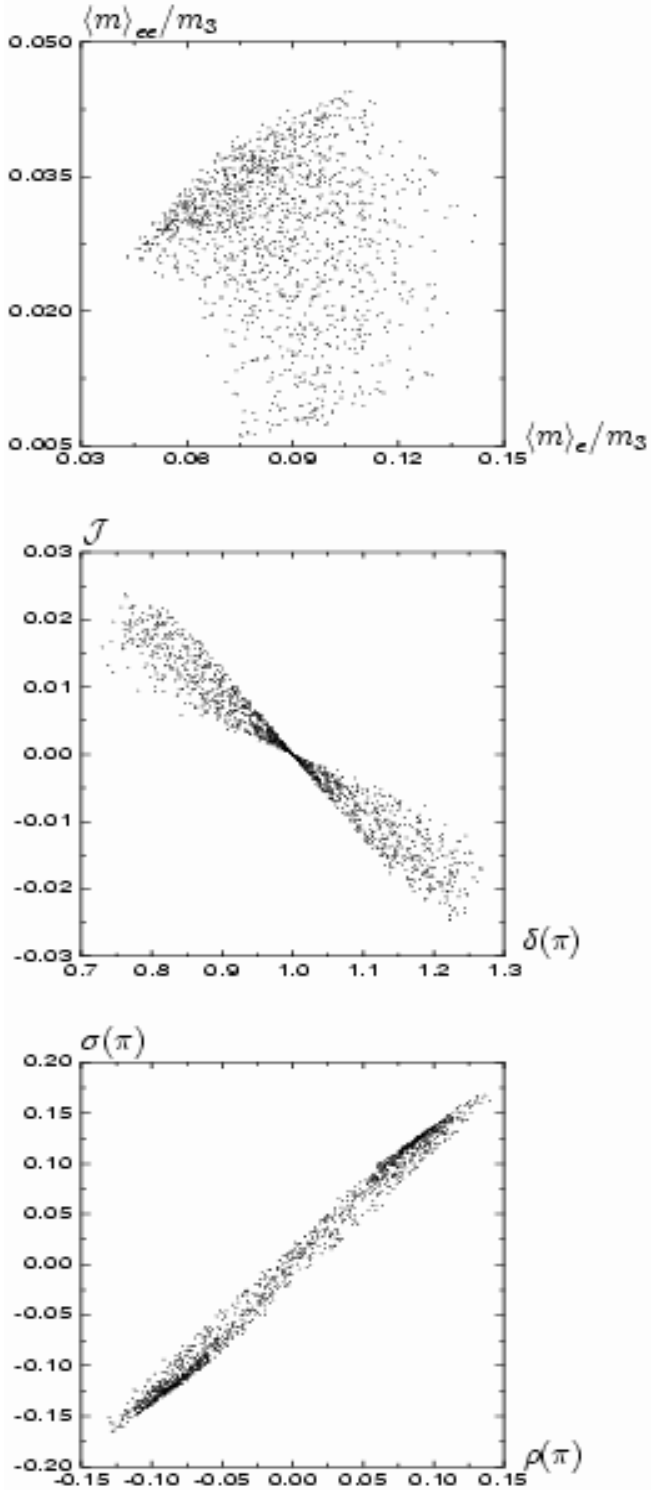

FIG. 15. A simple seesaw example: the outputs of $(\langle m \rangle_e, \langle m \rangle_{ee})$, $(\delta, \mathcal{J})$ and (ρ, σ) at the 2σ level.